JACC: CARDIOVASCULAR IMAGING VOL. 12, NO. 1, 2019
© 2019 BY THE SOCIETY OF CARDIOVASCULAR COMPUTED TOMOGRAPHY
AND THE AMERICAN COLLEGE OF CARDIOLOGY FOUNDATION
PUBLISHED BY ELSEVIER

GUIDELINES

Computed Tomography Imaging in the Context of Transcatheter Aortic Valve Implantation (TAVI)/Transcatheter Aortic Valve Replacement (TAVR)

An Expert Consensus Document of the Society of Cardiovascular Computed Tomography

Philipp Blanke, MD,[a] Jonathan R. Weir-McCall, MBChB, PhD,[b] Stephan Achenbach, MD,[c] Victoria Delgado, MD, PhD,[d] Jörg Hausleiter, MD,[e] Hasan Jilaihawi, MD,[f] Mohamed Marwan, MD,[c] Bjarne L. Nørgaard, MD, PhD,[g] Niccolo Piazza, MD, PhD,[h] Paul Schoenhagen, MD, PhD,[i] Jonathon A. Leipsic, MD[a]

1. PREAMBLE/INTRODUCTION

Since the publication of the first expert consensus document on computed tomography imaging before transcatheter aortic valve implantation (TAVI)/transcatheter aortic valve replacement (TAVR) by the Society of Cardiovascular Computed Tomography (SCCT) in 2012 (1), there has been tremendous advancement in the field. Significant technological advancements and a wealth of trial data have led to deep integration of TAVI/TAVR and CT Imaging into clinical practice. The indications for TAVI/TAVR as the treatment strategy for patients with symptomatic severe aortic stenosis (AS) has expanded from those who are ineligible for surgery or high risk surgical candidates to also now include those at intermediate risk for conventional surgical valve replacement (2-6).

Advances in non-invasive imaging have supported growth and maturation of the field. Clinical outcomes have improved based on the thoughtful integration of advanced non-invasive imaging into patient selection, treatment planning, device selection, and device positioning. While computed tomography (CT) was initially used primarily for the assessment of peripheral access, the role of CT has grown substantially and CT is now the gold standard tool for annular sizing, determination of risk of annular injury and coronary occlusion, and to provide co-planar

From the [a]Department of Radiology, St Paul's Hospital & University of British Columbia, Vancouver, British Columbia, Canada; [b]Department of Radiology, University of Cambridge, Addenbrooke's Hospital, Cambridge, United Kingdom; [c]Department of Cardiology, Friedrich-Alexander-University Erlangen-Nürnberg, Erlangen, Germany; [d]Department of Cardiology, Heart Lung Center, Leiden University Medical Center, Leiden, the Netherlands; [e]Medizinische Klinik und Poliklinik I der Ludwig-Maximilians-Universität München, Munich, Germany; [f]New York University Medical Center, New York, New York; [g]Department of Cardiology, Aarhus University Hospital, Aarhus, Denmark; [h]McGill University Health Centre, Montreal, QC, Canada; and the [i]Imaging Institute and Heart&Vascular Institute, Cleveland Clinic Lerner College of Medicine, Cleveland, Ohio.
This paper will be copublished in the *Journal of the Cardiovascular Computed Tomography*.
Dr. Blanke is a consultant for Edwards Lifesciences and Circle Cardiovascular Imaging; and provides CT core lab services for Edwards Lifesciences, Medtronic, Neovasc, and Tendyne Holdings, for which he receives no direct compensation. Dr. Delgado receives speaker fees from Abbott Vascular; and has received departmental unrestricted research grants from Medtronic, Biotronik, Edwards Lifesciences, GE Healthcare, and Boston Scientific. Dr. Hausleiter has received speaker honoraria from Abbott Vascular and Edwards LifeSciences. Dr. Jilaihawi has acted as a consultant for Edwards Lifesciences; and received research grants from Medtronic and Abbott Vascular. Dr. Marwan has received speaker honoraria from Siemens Healthcare and Edwards Lifesciences. Dr. Norgaard has received unrestricted institutional research grants from Edwards Lifesciences, Siemens, and HeartFlow. Dr. Piazza is a clinical proctor and consultant for, has received research grants from, and serves on an advisory board and steering committee for Medtronic. Dr. Leipsic serves as a consultant and has stock options in HeartFlow and Circle Cardiovascular Imaging; and receives speaking fees from GE Healthcare. All other authors have reported that they have no relationships relevant to the contents of this paper to disclose.

ISSN 1936-878X/$36.00 https://doi.org/10.1016/j.jcmg.2018.12.003

Descargado para Anonymous User (n/a) en Consejeria de Sanidad de Castilla y Leon(Sacyl) de ClinicalKey.es por Elsevier en marzo 05, 2019.
Para uso personal exclusivamente. No se permiten otros usos sin autorización. Copyright ©2019. Elsevier Inc. Todos los derechos reservados.

fluoroscopic angle prediction in advance of the procedure. Further benefits of cardiac CT have also been demonstrated in the follow-up of TAVI/TAVR for assessment of post-procedural complications including identification of leaflet thickening (7,8).

Since the last SCCT consensus statement, there has been a substantial volume of new data published describing the use of CTA in TAVI/TAVR planning and post-procedural assessment. This updated consensus statement has been written to better reflect the data now available. The content and recommendations of this document reflect an expert consensus taking into consideration all published literature, but is not in itself a systematic review. For recommendations, level of consensus was graded as strong (≥9 in agreement out of the 11 members of the writing group), moderate (7 to 8) and weak (6). Any recommendations with less than 6 of the author group in support of the statement were not adopted into this expert consensus document.

2. CT DATA ACQUISITION AND RECONSTRUCTION

Data acquisition strategies and scanning protocols vary depending on scanner manufacturer, system, and institutional preferences (9). This document provides recommendations for reliable CT image acquisition for TAVI/TAVR planning. The key component of all approaches is an ECG-synchronized computed tomographic angiography (CTA) data set that covers at least the aortic root in order to provide artifact free anatomical information of the aortic root, followed by a commonly non-ECG synchronized CTA data acquisition of the aorto/ilio/femoral vasculature for assessment of the access vasculature. Ideally, both acquisitions are combined in a comprehensive scanning protocol with a single contrast administration. The sequence of patient preparation and the relevant principles of CT data acquisition will be explained in brief below.

2.1. SCAN STRATEGY AND SCAN COVERAGE. In general, two different approaches are used to combine the ECG-synchronized data set of the aortic root structures and the non-ECG-synchronized computed tomography angiography (CTA) of the aorto/ilio/femoral vasculature into one comprehensive acquisition protocol:

1) Cardiac ECG-synchronized data set of the aortic root and heart followed by a non-ECG-synchronized CTA of the thorax, abdomen, and pelvis. Although this approach can result in repeat data acquisition of the aortic root and cardiac structures, the time-intensive ECG-synchronized data acquisition is kept to a minimum, allowing for a reduction of the overall contrast dose. Furthermore, limiting the ECG-synchronized data acquisition decreases the radiation dose-intensive portion of the examination, despite parts of the scan range possibly being covered twice. The ECG-synchronized data set should at least cover the aortic root, but can include the entire heart.
2) ECG-synchronized data acquisition of the thorax followed by a non-ECG-synchronized CTA of the abdomen and pelvis. A disadvantage of this approach is the higher radiation dose, and the relatively long acquisition time required for the entire thorax with potential need for larger contrast dose and risk of breathing artifacts.

The scanner hardware employed may further dictate which of these approaches is employed.

2.2. ECG-SYNCHRONIZED CTA OF THE AORTIC ROOT AND HEART: ACQUISITION TECHNIQUE. The selected acquisition mode as well as exposure settings should account for dynamic changes of aortic root geometry and dimensions throughout the cardiac cycle. Given that aortic root dimensions are commonly larger in systole (10,11), and that most sizing algorithms for transcatheter heart valves are based on systolic dimensions, systolic scan coverage is recommended. However, diastolic information may be valuable for evaluation of aortic valve morphology and rarely, the largest dimensions of the annulus may occur in diastole in the setting of inversed dynamism in septal hypertrophy (11–13). For that reason, image acquisition covering the entire cardiac cycle should be considered. This wider phase of acquisition offering systolic and diastolic data may be particularly useful if systolic reconstructions are degraded by artifact. Scan coverage should at least include the aortic root but coverage of the entire heart is beneficial.

For CT systems with limited detector coverage, i.e., systems that cannot cover the entire aortic root within one rotation, retrospective ECG-gating allows coverage of the entire cardiac cycle, while offering most flexibility regarding data salvage by means of ECG-editing. Dose-modulation may be used to mitigate the high radiation exposure, with peak tube current applied during at least systole. However, tube current outside of the peak acquisition window should be maintained to such a level as to allow for characterization of the aortic annulus and valve. Prospective ECG-triggering may constitute an alternative. However, this technique is more susceptible to step-artifacts in the setting of increased heart rate variability (e.g. premature contractions, atrial fibrillation) with the risk of rendering images inadequate

Descargado para Anonymous User (n/a) en Consejeria de Sanidad de Castilla y Leon(Sacyl) de ClinicalKey.es por Elsevier en marzo 05, 2019.
Para uso personal exclusivamente. No se permiten otros usos sin autorización. Copyright ©2019. Elsevier Inc. Todos los derechos reservados.

TABLE 1 Preferred Mode of Acquisition for ECG-Synchronized CTA of the Aortic Root Stratified by Scanner System

Manufacturer	Scanner Geometry	Preferred Acquisition Mode
GE	64-row family	Spiral/helical acquisition with retrospectively ECG-gated image reconstruction
	Revolution (256 row)	Prospectively ECGgated, axial one beat acquisition
Philips	All scanners	Spiral/helical acquisition with retrospectively ECG-gated image reconstruction
Siemens	All scanners	Spiral/helical acquisition with retrospectively ECG-gated image reconstruction
Toshiba	64/80-row family	Spiral/helical acquisition with retrospectively ECG-gated image reconstruction
	Aquilion One (320/640 row)	Prospectively ECGgated, axial one beat acquisition

for quantitative analysis, and does not allow for image salvage by means of ECG-editing. If employed, the acquisition window should be kept wide to cover at least systole.

For systems with whole-heart coverage (i.e., 16-cm detector coverage), an ECG-gated one beat acquisition should be employed. Peak tube current should be applied at least during systole, with consideration for coverage of the entire cardiac cycle. Recommended acquisition mode for employed scanner systems are listed in **Table 1**.

Other acquisition settings, in particular tube voltage and tube current settings should follow institutional policies and preferences but should allow for acquisition of image data with sufficiently low image noise to ensure fully diagnostic image quality in thin-slice reconstructions. Guidance on acquisition settings is outlined in the 'Radiation parameters' section below (9). In centers with multiple scanners, matching the most complex patients (such as those with arrhythmias, cardiac failure, or chronic kidney disease) to higher specification scanners (such as those with whole heart coverage, or dual sources) should be considered (14).

2.3. NON-ECG SYNCHRONIZED CTA OF THE AORTO/ILIO/FEMORAL VASCULATURE: ACQUISITION TECHNIQUE. The CTA of the aorto/ilio/femoral vasculature should extend from the upper thoracic aperture to the lesser trochanter to include the thoracic and abdominal aorta, the iliac arteries and common femoral arteries, the latter constituting the most common vascular access site. For a more comprehensive evaluation the scan range can be extended cephalad to fully include the subclavian arteries for assessment of this alternative access route (15). Most commonly, this CTA is performed employing a helical, non-ECG synchronized data acquisition immediately following the ECG-synchronized data set of the aortic root. Other acquisition settings, in particular tube voltage and tube current settings should follow institutional policies and preferences, but should allow for acquisition of image data with sufficiently low image noise to ensure fully diagnostic image quality in thin-slice reconstructions. Most scanner systems require a brief intermission between the ECG-synchronized and non-synchronized data acquisition to reposition the table and adjust scan settings. This needs to be accounted for by the contrast administration protocol in order to allow for sufficient contrast attenuation of the aorto/ilio/femoral vasculature.

2.4. RADIATION PARAMETERS AND CONSIDERATIONS. Acquisition parameters should employ the 'As low as reasonably achievable' (ALARA) principle (9). According to recommendations on radiation protection in cardiovascular CT by the Society of Cardiovascular Computed Tomography (SCCT), a tube potential of 100 kV should be considered for patients weighing ≤90 kg or with a body mass index (BMI) ≤30 kg/m^2; whereas a tube potential of 120 kV is usually indicated for patients weighing >90 kg and with a BMI > 30 kg/m^2 (9). Tube current should be adjusted, based on individual patient's size, to the lowest setting that guarantees acceptable image noise (9). Expected increase in image noise with lower tube current can be mitigated with the use of iterative image reconstruction. The majority of commercially available scanner systems provide software algorithms to automatically adjust exposure parameters to the patient's body habitus within defined boundaries.

To date, patients being treated with TAVI/TAVR have predominantly been septuagenarians and octogenarians with the mean age of patients receiving TAVI/TAVR being 79.8 to 83.6 years in high and intermediate risk trials, 79.1 years in the all comer NOTION trial and 80.1 years in the low risk OBSERVANT registry with mean age not expected to drop below 75 years of age in low risk cohorts (4–6,16,17). As a result the primary concern for the imaging protocol should be to ensure diagnostic quality images, and to minimize the need for repeat CTA and repeat contrast administration. In case of younger patients, the most effective mode for reducing radiation dose is to minimize the scan volume performed using ECG-synchronization as well as limiting the peak dose coverage when using dose modulation. Prospectively triggered acquisitions focusing on systole can be

Descargado para Anonymous User (n/a) en Consejeria de Sanidad de Castilla y Leon(Sacyl) de ClinicalKey.es por Elsevier en marzo 05, 2019.
Para uso personal exclusivamente. No se permiten otros usos sin autorización. Copyright ©2019. Elsevier Inc. Todos los derechos reservados.

TABLE 2 Recommendations for IV Contrast Administration

Parameter	Recommendation
Iodine concentration	Iodinated contrast agent as per institutional standards
Flow rate	4–6 ml/s
Volume	As per institutional standard for routine coronary cardiac CT, commonly 50–100 cc
IV-access	Antecubital vein
Timing	Bolus tracking to allow for peak contrast in the ascending aorta (may vary with scanning system used)

considered a reasonable alternative particularly in patients with lower and regular heart rates.

2.5. CONTRAST ADMINISTRATION. Intravenous contrast administration is required for assessment of the aortic root anatomy and peripheral vasculature. In particular accurate identification of the annular plane and contour, as well as accurate evaluation of the access route requires sufficient contrast enhancement. Optimal images require high intra-arterial opacification, and attenuation values should exceed 250 Hounsfield units (9).

Use of dual head injector and antecubital IV access is recommended. Timing of contrast administration and the start of the ECG-synchronized data acquisition should be achieved using bolus tracking with a region of interest in the ascending aorta, although variation occurs with the specific scanner system employed. Flow rates of 4 to 6 ml/s commonly result in sufficient contrast attenuation, but should be adjusted to both, body habitus and iodine concentration of the contrast agent employed (Table 2). Total contrast volume commonly varies between 50 and 100 cc, with higher volumes needed in larger patients and in older CT scanners with lower Z-axis coverage. In general, optimization of the comprehensive scanning protocol for the scanning system employed allows for lower overall contrast volumes (see Table 3).

In patients with impaired kidney function total amount of contrast should be reduced to a minimum while still ensuring sufficient contrast attenuation. This can be achieved using lower flow rates as low as 3 ml/s, low tube potential (down to 80kVp), multiphasic contrast injection protocols and diligent optimization of the scanning protocol and timing (18,19). Prospective high pitch imaging is an alternative useful adjunct to low contrast dose whilst maintaining image quality (20).

2.6. PATIENT PREPARATION. Patients should be instructed to maintain an adequate fluid intake prior to the examination. In patients with eGFR ≥30 ml/min/1.73 m^2, even in the presence of concomitant risk factors, a regime of no prophylaxis has been shown to be non-inferior to IV hydration for the prevention of acute kidney injury (21). In cases with severe renal impairment, cautious pre-scan intravenous hydration may be beneficial and should be considered according to institutional protocols (22).

For administration of iodinated contrast, at least a 20-gauge intravenous access should be placed, preferably in an antecubital vein. Although elevated heart rates may negatively affect image quality, in particular when using single-source systems, it is not recommended to perform routine heart rate control with beta blockade, given the risk of potential side effects in patients with severe aortic stenosis. Administration of sublingual nitrates in patients with significant AS is contraindicated.

2.7. NON-CONTRAST CARDIAC CT. Non-contrast evaluation of the aortic root is not an essential component of the TAVI/TAVR work-up, but may have utility in

TABLE 3 Summary of Recommendations for CT Acquisition Prior to TAVI/TAVR

Recommendation	Grade of Recommendation*
The imaging volume should include the aortic root, aortic arch and ilio-femoral access	Strong
Imaging of the aortic root should be performed using ECG-synchronized acquisition	Strong
Imaging of the aorta and iliofemoral vessels can be performed without ECG synchronization	Strong
Choice of acquisition mode should be tailored according to available scanner technology	Strong
CT acquisitions should focus on optimization of image quality while in accordance with ALARA principles	Strong
Thin slice collimation and reconstructed slice thickness ≤1 mm for the root and ≤1.5 mm for the peripheral vasculature should be obtained and used.	Strong
In patients with an eGFR ≥30 ml/min/1.73 m^2 no pre hydration is required	Weak
In patients with eGFR <30 ml/min/1.73 m^2 reduction of iodinated contrast volume and prehydration may be considered	Strong
Routine use of beta blockade is not recommended.	Strong
Beta blocker use may be considered in selected cases and should be used cautiously with careful clinical oversight	Strong
Use of nitroglycerin is contra-indicated	Strong

*Based on level of consensus.

ALARA = as low as reasonably achievable; ECG = electrocardiogram; eGFR = estimated glomerular filtration rate; CT = computed tomography; TAVI = transcatheter aortic valve implantation; TAVR = transcatheter aortic valve replacement.

Descargado para Anonymous User (n/a) en Consejeria de Sanidad de Castilla y Leon(Sacyl) de ClinicalKey.es por Elsevier en marzo 05, 2019.
Para uso personal exclusivamente. No se permiten otros usos sin autorización. Copyright ©2019. Elsevier Inc. Todos los derechos reservados.

the setting of uncertain AS severity where the aortic valve calcium score is known to correlate well with aortic stenosis severity (23). This is of most use in suspected low-flow low-gradient AS in those with either a preserved or reduced ejection fraction with no flow reserve on dobutamine stress echocardiography (24). In this situation, the calcium score of the valve can be used to adjudicate the presence or absence of severe aortic stenosis (25). CT acquisition for the assessment of aortic valve calcification should be performed using the same acquisition parameters used for assessment of the coronary artery calcium score although further studies are underway to determine thresholds for post-contrast CT scans (26,27). The valvular calcification is then contoured utilizing standard coronary artery calcium scoring software, with contours applied around the valvular calcification, ensuring the exclusion of aortic wall, left ventricular outflow tract (LVOT) or coronary calcification. Sex-specific thresholds are utilized, with an Agatston score of ≥3,000 in men and ≥1,600 in women making severe aortic stenosis very likely, while an Agatston score of <1,600 in men and <800 in women makes it highly unlikely (24). Non-contrast cardiac CT should not be used for annular sizing due to the inability to identify the cusp hinge points and thus the inability to accurately and reproducibly define the annular plane.

2.8. RECONSTRUCTION TECHNIQUE. ECG-synchronized CT data should be reconstructed as an axial, thin-sliced multiphasic data set, also referred to as 'cine', 'functional' or '4D-CT'. Multiphasic data sets should be reconstructed with <1mm slice thickness using a small reconstruction field of view encompassing only the cardiac structures and a 512×512 matrix in order to optimize spatial resolution. Prior to image reconstruction, the ECG-tracing should be manually reviewed to ensure correct R-peak identification by the scanning system, with manual correction if required. When using retrospective ECG-gating, ECG-editing should be considered to reduce artifacts in the setting of increased heart rate variability, e.g., in premature contractions or atrial fibrillation. For relative image reconstruction, reconstruction interval should be spaced at ≤10% intervals across the acquired portion of the cardiac cycle. Alternatively, if available on the employed scanning system, multiphasic data sets can be reconstructed using absolute image reconstruction at 50msec increments, which result in superior image quality in patients with increased heart rate variability such as in atrial fibrillation (28,29).

The non-ECG synchronized CTA of the aorto/ilio/femoral vasculature should be reconstructed as an axial data set with ≤1.5 mm slice thickness in a contiguous or overlapping fashion, using a large field of view and either filtered back projection or iterative reconstruction.

3. AORTIC ROOT: ANATOMICAL DEFINITIONS AND ASSESSMENT

Precise understanding and assessment of the anatomy of the aortic valvular complex is crucial to achieve optimal sizing of transcatheter heart valves (THV) as well as to identify patients at increased anatomical risk for adverse events such as coronary artery occlusion. The aortic root is an extension of the left ventricular outflow tract, extending from the basal attachment of the aortic valve cusps within the LVOT to their peripheral attachment at the level of the sinotubular junction. Its components are the sinuses of Valsalva, the fibrous interleaflet triangles and the valvular cusps themselves (30,31).

3.1. AORTIC ANNULUS: DEFINITIONS AND MEASUREMENT TECHNIQUES. For the purpose of anatomical sizing in the context of TAVI/TAVR, the aortic annulus is defined as the luminal contour within a virtual plane aligned with the most basal attachment points of the three aortic valve cusps (sometimes referred to as the 'basal hinge points'). Quantitative assessment requires the accurate identification of each of these three points in turn to create a plane that transects all three.

Identification and positioning of the annular plane can be performed:

1. Manually, using standard multiplanar reformats, the technique for which is shown in **Figure 1**.
2. Using a software-based facilitating workflow with manual identification of the basal hinge points by placing marker points with subsequent positioning of the plane by the software.
3. Semi-automatically, by means of automated software-based anatomical segmentation, with verification by a trained observer and manual correction where required.

While facilitated or semi-automated workflows may be used, the interpreter analyzing the imaging must confirm the accuracy of the generated annular plane and perform manual corrections if required. For a summary of recommendations please see **Table 5**.

For quantification of annular dimensions, various measurement tools are available across software platforms (**Fig. 2**):

1. Cubic spline interpolation: Manually placed segmentation points which are automatically connected by a cubic spline interpolation.

Descargado para Anonymous User (n/a) en Consejeria de Sanidad de Castilla y Leon(Sacyl) de ClinicalKey.es por Elsevier en marzo 05, 2019.
Para uso personal exclusivamente. No se permiten otros usos sin autorización. Copyright ©2019. Elsevier Inc. Todos los derechos reservados.

FIGURE 1 **Identifying the Annular Plane in Aortic Valves With Tricuspid Morphology**

Step & Description	Multiplanar reformats
Step 1: Start out with multi-planar images in default axial, sagittal, and coronal orientation; center cross-hairs onto the aortic valve	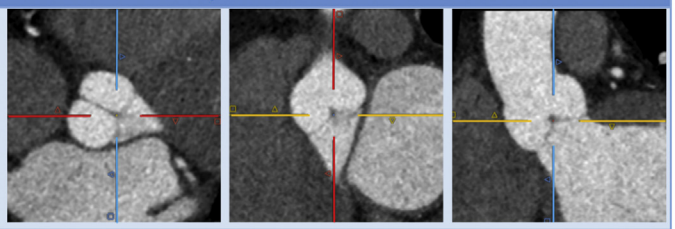
Step 2: Align the cross-hairs in the sagittal and coronal views with the long axis of the aortic root; the resulting double oblique transverse view will depict the aortic valve en face.	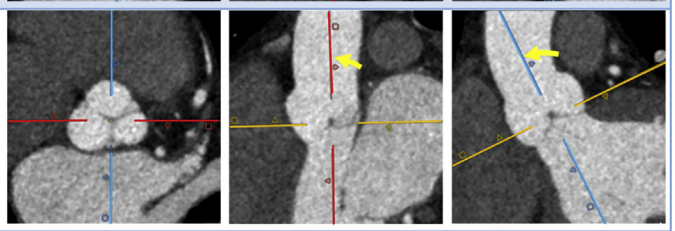
Step 3: Move the double oblique transverse plane up and down to identify the lowest insertion point of the right coronary cusp which is usually located at about 1 o´clock. Position the center of the cross-hairs exactly at the most basal insertion point of the right coronary cusp (white arrow head).	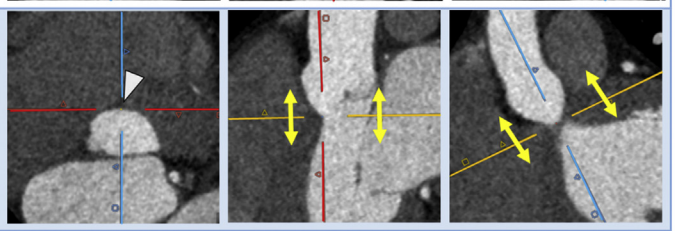
Step 4: Rotate the cross-hairs counter-clock-wise without moving up and down while maintaining its center position so that the formerly coronal view (here red cross-hair) transects the lowest insertion point of the non-coronary cusp, which is located at approximately 8 o´clock (white arrow head).	
Step 5: The formerly coronal, now double-oblique view will show the lowest insertion point both of the right coronary cusp and the non-coronary cusp (white arrow heads). In this view, rotate the (here orange) cross-hair indicating the double-oblique transverse view to transect exactly through the most basal insertion point of the non-coronary cusps. Once this is achieved, the transverse double oblique plane will contain two of the three lowest cusp insertion points.	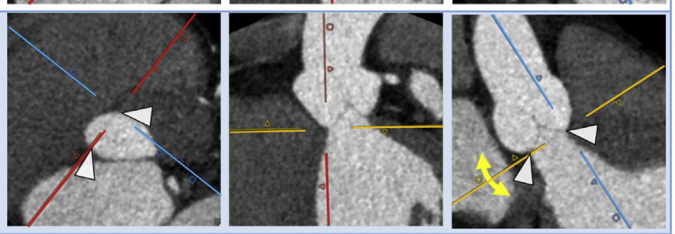
Step 6: In the formerly sagittal view, rotate (without moving it) the cross-hair of the transverse double oblique plane (here orange) until the lowest insertion point of the left coronary cusp just barely appears in the double oblique transverse view (white arrow head). Now, the formerly axial plane is exactly aligned with the lowest cusp insertion points of all three aortic cusps and represents both the orientation as well as the level of the annular plane.	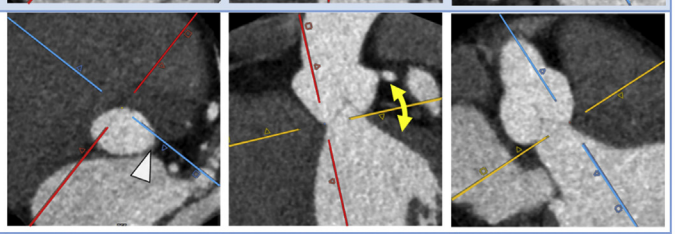
Step 7: Measurements of aortic annulus dimensions should be performed in the annular plane by means of a contouring tool.	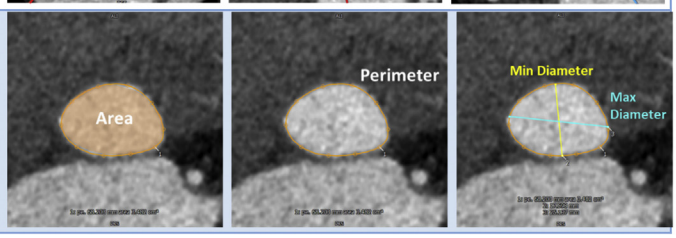

Descargado para Anonymous User (n/a) en Consejeria de Sanidad de Castilla y Leon(Sacyl) de ClinicalKey.es por Elsevier en marzo 05, 2019.
Para uso personal exclusivamente. No se permiten otros usos sin autorización. Copyright ©2019. Elsevier Inc. Todos los derechos reservados.

FIGURE 2 **Contouring Tools for Annular Segmentation**

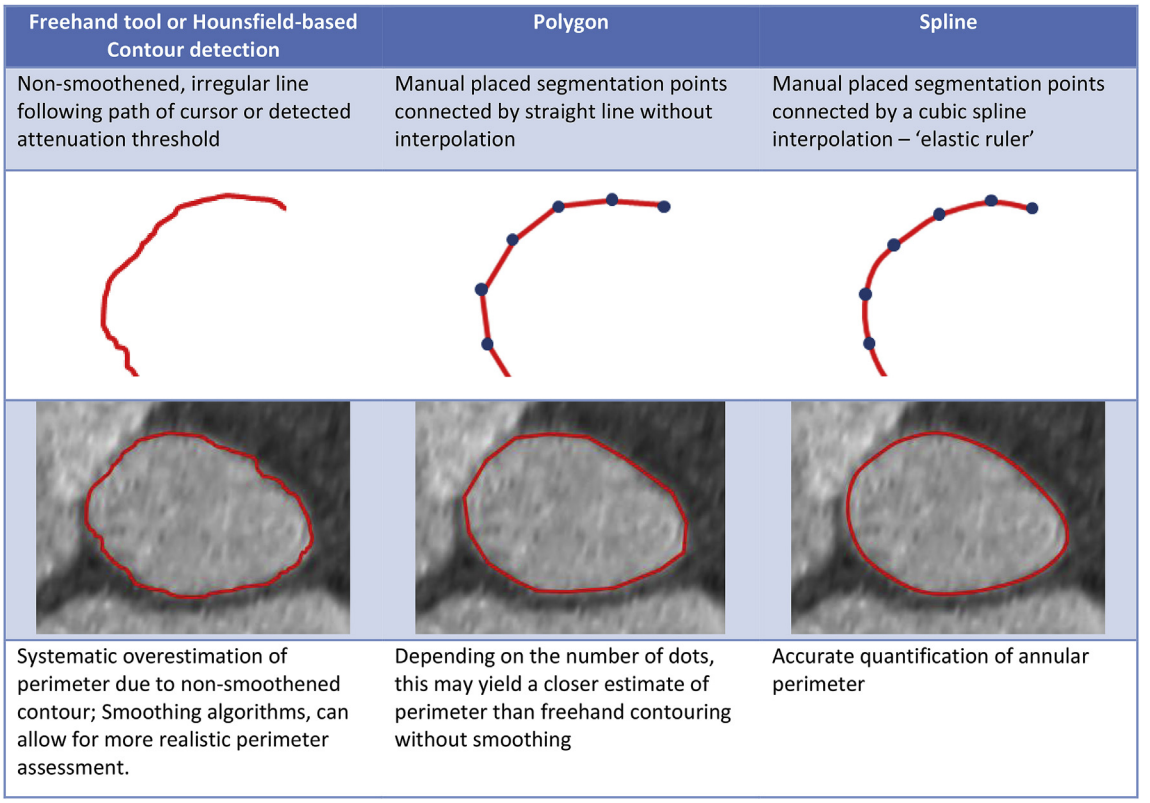

2. Polygon: Manually placed segmentation points which are automatically connected by straight lines.
3. Attenuation/Hounsfield unit based contour detection.
4. Freehand contour: The annular contour is traced manually with the cursor.

All techniques commonly provide the annular area in either [mm^2] or [cm^2]. Cubic spline interpolation commonly provide also the annular perimeter in [mm]. Polygon tools may underestimate the annular perimeter when compared to cubic spline interpolation, given the straight line connection of the segmentation points. Attenuation/Hounsfield unit based contour detection as well as freehand contour techniques may, depending on the software platform, result in jagged contours, artificially increasing the reported perimeter. For this reason, smoothing algorithms may be used to create a rather spline-like contour. Perimeter values should only be reported when using these measurement tools, if the contour is smoothened.

Most contouring tools provide short and long axis dimensions in [mm] which are automatically derived by software algorithms, although methodology differ between platforms (e.g., perpendicular versus non-perpendicular orientation; intersection centric versus eccentric). Alternative, manual caliper measurements can be performed. Overall, short and long axis dimensions inform on the eccentricity of the annular cross-sectional dimensions. Importantly, manual caliper measurements should not be used to assess overall annular dimensions instead of contouring tools.

Independent of the measurement technique used, the annular contour should be drawn along the blood-pool tissue interface, carefully avoiding presence of any tissue within the contour and avoiding any contrast outside of the contour. In case of annular calcification, irrespective of crescent or protruding distribution, the contour should be drawn in a harmonic fashion as if no calcium is present, as this aids in measurement standardization.

3.2. ANNULAR DYNAMISM & PHASE SELECTION. During systole, conformational changes with decrease in ellipticity as well as stretch of the annular contour commonly result in a larger annular area and perimeter as compared to diastole (**Fig. 3**) (10,32). This annular dynamism has significant implications for

Descargado para Anonymous User (n/a) en Consejeria de Sanidad de Castilla y Leon(Sacyl) de ClinicalKey.es por Elsevier en marzo 05, 2019.
Para uso personal exclusivamente. No se permiten otros usos sin autorización. Copyright ©2019. Elsevier Inc. Todos los derechos reservados.

FIGURE 3 Dynamic Changes of the Aortic Annulus Throughout the Cardiac Cycle

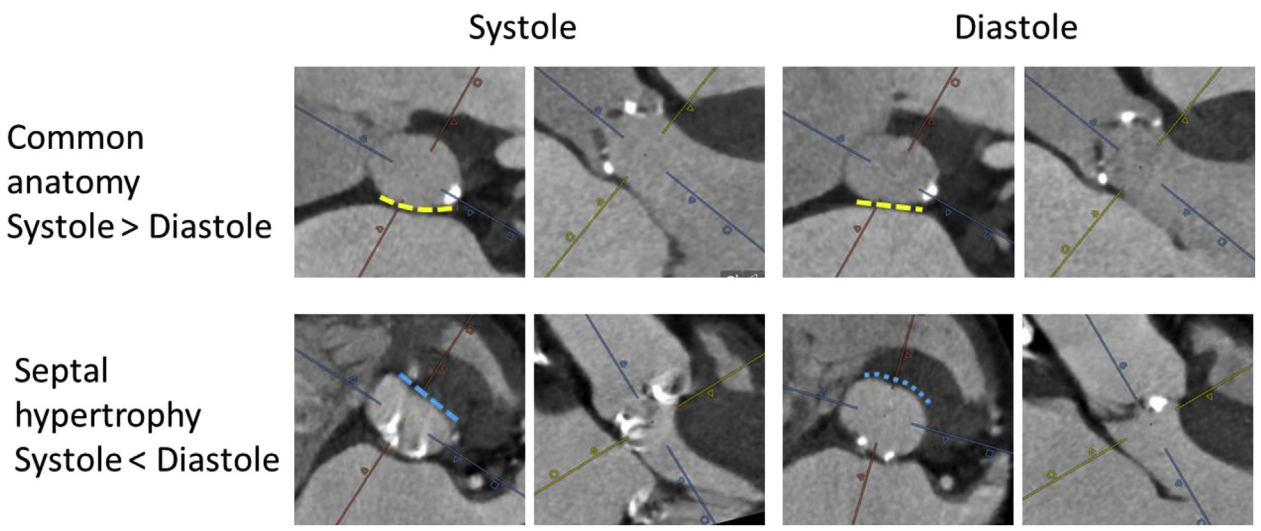

Example with common anatomy and regular dynamism **(upper row)**, demonstrating larger dimensions in systole than diastole, in parts due to bulging of the aortomitral continuity **(dashed yellow line)** towards the left atrium in systole and flattening in diastole. The lower row shows an example of septal hypertrophy with smaller annular dimensions in systole than diastole, in part due bulging of the basal septum **(dashed blue line)** into the annulus during systole.

sizing with the potential for unintended undersizing if sizing is based on diastolic assessment (12,33).

Annular measurements should be performed using the ECG-synchronized, ideally multiphasic dataset. Identifying the reconstruction phase with largest annular dimensions is important given the implications for device sizing. The annular anatomy should be reviewed throughout the available portion of the cardiac cycle and the phase yielding the largest dimensions with adequate image quality should be visually identified. Importantly, changes in the orientation of the annular plane throughout the cardiac cycle may require adjustment of the imaging plane. Care should be taken to identify a reconstruction phase with adequate image quality, ie. sharp depiction of the annular contour. Reconstruction phases with inadequate depiction of the annular contour, i.e., blur or double contours, should be avoided.

TABLE 4 Grading Scale for Image Quality for Assessment of the Aortic Root

Grade	Definition
Good (diagnostic)	• Sharp depiction of the annular contour with sufficient contrast attenuation in the absence of artifacts
Fair (diagnostic)	• Low contrast attenuation • Increased image noise • Mild motion artifacts, double contours or stair-step artifacts
Poor (non-diagnostic)	• Too low contrast attenuation • Excessive image noise • Excessive motion artifacts or double contours • Pronounced stair-step artifact transecting the annular contour

3.3. IMAGE QUALITY. Reliable quantification of aortic annular and aortic root dimensions requires adequate image quality defined by sharp depiction of the annular contour given sufficient contrast attenuation, noise preposition as well as absence of motion artifacts, double contours, or stair step artifacts. Image quality can be rated using a subjective, qualitative grading scale as good, fair and poor (non-diagnostic) (Table 4).

3.4. LANDING ZONE CALCIUM. The device landing zone comprises the valve cusps, aortic annulus and LVOT (34,35). It has been demonstrated that the presence of severe calcification of the LVOT and aortic valve is associated with increased risk of paravalvular regurgitation particularly when calcium protrudes into the LVOT (36-40). In clinical practice, the description of annular (within annular plane) and sub-annular (upper 4 to 5 mm of the LVOT where device gets into contact) calcification is almost exclusively performed in a subjective, qualitative fashion graded as none, mild, moderate, severe based on the circumferential extent, the depth of extension inferiorly into the LVOT and the thickness of the calcification projecting radially into the LVOT (Fig. 4). Annular and sub-annular calcification should be described as crescent/flat/adherent or protruding as well as its relation to the aortic cusps. The location of calcification within the LVOT varies significantly across severe aortic stenosis patients. The region

Descargado para Anonymous User (n/a) en Consejeria de Sanidad de Castilla y Leon(Sacyl) de ClinicalKey.es por Elsevier en marzo 05, 2019.
Para uso personal exclusivamente. No se permiten otros usos sin autorización. Copyright ©2019. Elsevier Inc. Todos los derechos reservados.

TABLE 5 Summary of Recommendations for the Sizing and Reporting of the Aortic Valve, Annulus and Outflow Tract

Recommendation	Grade of Recommendation*
Annulus assessment and planning	
While facilitated or semi-automated workflows may be used, the interpreter analyzing the imaging must be able to confirm the accuracy of the generated annular plane and perform manual corrections if required.	Strong
Systolic measurements are preferred for measurement and calculation of device sizing	Strong
Area and perimeter measurements are preferred for sizing of the aortic annulus over isolated 2 dimensional measurements and should be provided in the report	Strong
Landing zone calcification	
Annular and subannular calcification should be qualitatively described regarding morphology and extent as well as relation to the aortic valve cusps.	Strong
Valve morphology	
Number of cusps should be stated, and if a bicuspid valve is present, its morphology should be classified.	Strong
The presence of a median raphe and the absence/presence of calcification of this should be mentioned	Strong
The aortic annulus size should be measured and reported in bicuspid aortic valves as for tricuspid aortic valves.	Strong
Aortic root measurement	
Pre-TAVI/TAVR CT assessment should include coronary height, mean SOV diameter, and STJ height and diameter	Strong
Coronary ostial distance from aortic annulus should be measured in a perpendicular fashion from the established annular plane	Strong

*Based on level of consensus.

CT = computed tomography; SOV = sinus of valsalva; STJ = sinotubular junction; TAVI = transcatheter aortic valve implantation; TAVR = transcatheter aortic valve replacement.

below the non-coronary and the left coronary cusps, including the intervalvular fibrosa, is most frequently affected. Large protruding nodules of calcification may increase the risk of annular rupture particularly with balloon expandable valves and should thus be specifically mentioned in the report (34). Finally, the device landing zone is in close spatial relationship with the conduction system which may be compressed and damaged, causing atrioventricular block and need for pacemaker implantation especially in the context of severe calcification of the subannular device landing zone, with this effect amplified in the presence of pre-existent right bundle branch block (41,42). Unusual findings with regard to these variables should be included in the report.

3.5. VALVE MORPHOLOGY: DEFINITION AND MEASUREMENT TECHNIQUES. Bicuspid aortic valves (BAV) are found in up to 6% of patients presenting for TAVI/TAVR, and are associated with lower device success rates and higher rates of paravalvular regurgitation, but similar outcomes (43,44). Numerous classifications of BAV morphology exist including that of Sievers and Schmidtke (45) (which essentially focuses on the number of raphes (0, 1 or 2 for the respective types). More recently, a TAVI/TAVR-directed simplified BAV classification has been proposed. It distinguishes BAV morphology regarding (a) number of commissures (two vs. three) and (b) presence or absence of a raphe, yielding 3 broad morphologies: 1) tricommissural, in clinical routine often referred to as 'functional' or 'acquired' BAV (not part of Sievers classification); 2) bicommissural raphe-type (equivalent to Sievers Type 1); and 3) bicommissural non raphe-type (equivalent to Sievers Type 0) (**Fig. 5**) (47). Ascending aortic dilation and aneurysms are less common in 'tricommissural' BAV than 'bicommissural' BAV. Within 'bicommissural' BAV, the non-raphe type BAV typically exhibits larger sinus diameters despite smaller annuli. For bicommissural raphe-type BAV, raphe characteristics may also be described qualitatively and quantitatively including raphe length and raphe calcium (47).

Valve morphology should be systematically characterized and reported in all pre-TAVI/TAVR CT reports. Further, the degree of raphe calcification should be reported, e.g. using a qualitative scale (mild, moderate, severe), as severe raphe calcification may relate to higher likelihood of paravalvular regurgitation (44).

Defining the annulus may be a challenge in BAV, particularly in Sievers Type 0 BAVs where there are only two hinge points to define the annular plane. The technique used for tricuspid aortic valves therefore frequently needs to be adjusted as detailed in **Figure 6**. The annulus size should be measured and reported in the same fashion for BAV as for tricuspid aortic valves. The ascending aorta should also be examined in BAV due to the association between BAV and aortopathy (46).

3.6. CORONARY OSTIAL HEIGHT AND SINUS OF VALSALVA ASSESSMENT. Coronary occlusion is a feared complication of TAVI/TAVR which, while relatively rare with an incidence of 0.66%, is associated with a poor clinical outcome with a reported 30

Descargado para Anonymous User (n/a) en Consejeria de Sanidad de Castilla y Leon(Sacyl) de ClinicalKey.es por Elsevier en marzo 05, 2019.
Para uso personal exclusivamente. No se permiten otros usos sin autorización. Copyright ©2019. Elsevier Inc. Todos los derechos reservados.

FIGURE 4 Qualitative Grading of Annular/Sub-Annular and Left Ventricular Outflow Tract Calcification

Grade		Examples
Mild	Single, adherent, non-protruding focus of calcification	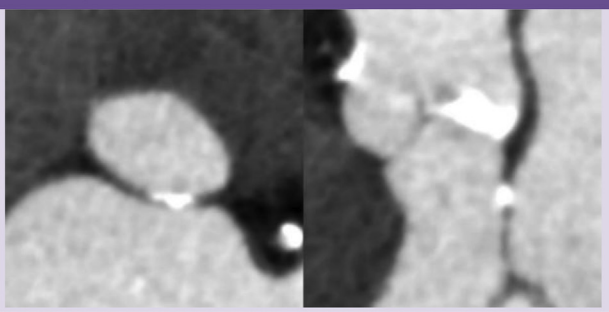
Moderate	Two or more nodules of calcification or a single nodule with limited protrusion into the annular/subannular lumen	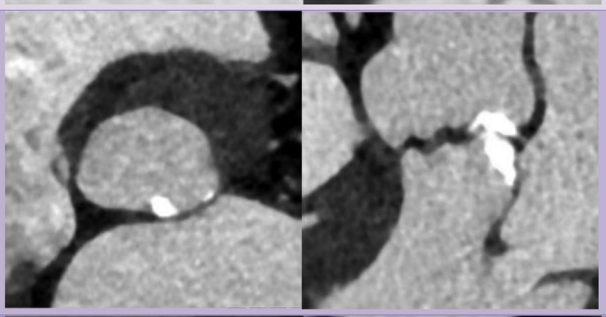
Severe	Single or multiple nodules of calcification, protruding into the annular lumen, and/or extending into the LVOT.	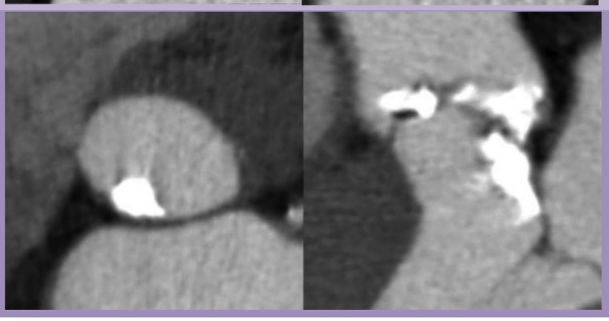

day mortality of up to 40.9% (48,49). CT is well established as the pre-procedural imaging gold standard for the determination of the risk of coronary occlusion. Low coronary ostial height (<12 mm) from the annulus and sinus of Valsalva mean diameter <30 mm connote an increased risk of coronary occlusion. However, it should be noted that there is no absolute threshold at which the procedure should be considered contra-indicated, given the relatively low specificity of these measurements (48), and thus coronary ostial height should not be considered as an isolated measure of risk of occlusion. Rather, the derived values for coronary height and sinus of Valsalva width should be interpreted in the context of annular dimensions, overall root dimensions and the anticipated THV size.

To ensure reproducibility the coronary ostial height should be measured in a perpendicular fashion to the annular plane using an electronic caliper tool from the annular plane to the lower edge of the coronary artery ostium, yielding a value in [mm] (**Fig. 7**). Sinus of valsalva diameter should be measured cusp to commissure in parallel to the annular plane using three caliper measurements in [mm]. For symmetric sinus of Valsalva anatomies, the three values can be averaged (**Fig. 7**). There is no recommendation as to whether these measurements are to be performed in systole or diastole. The SOV diameter and coronary artery heights should be included in the report.

3.7. SINOTUBULAR JUNCTION. Sinotubular (STJ) diameter and height are relevant to identify anatomies in which the anticipated THV may potentially get into contact with the STJ. In particular when using balloon-expandable devices in low STJ height anatomies, STJ diameter should be compared to the anticipated THV size in order to identify anatomies with smaller STJ diameter than THV diameter, which would be indicative of increased risk for STJ injury.

Descargado para Anonymous User (n/a) en Consejeria de Sanidad de Castilla y Leon(Sacyl) de ClinicalKey.es por Elsevier en marzo 05, 2019.
Para uso personal exclusivamente. No se permiten otros usos sin autorización. Copyright ©2019. Elsevier Inc. Todos los derechos reservados.

FIGURE 5 The Heterogeneous Spectrum of Bicuspid Aortic Valve Morphology

Classification	Characteristics	Double oblique transverse MPR	Volume rendered en face view systole	Volume rendered en face view diastole
Sievers Type 0/ bicommissural non-raphe type	• Two fairly symmetric cusps and two commissures • Each cusp has one most basal insertion point; thus there is a total of two most basal insertion points		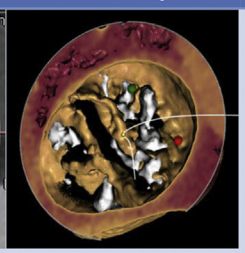	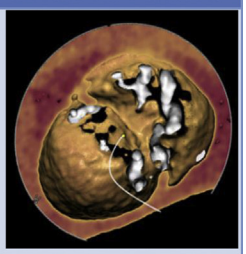
Sievers Type 1/ bicommissural raphe type	• Two of three cusps are conjoined by a raphe • Asymmetric cusp sizes with the cusp opposing the raphe (i.e. cusp not participating in raphe formation) being larger than in a tricuspid aortic valve • Raphe does not extend to the level of the STJ which is the distinguishing characteristics to a non-opening commisure • Size of raphe and degree of calcification can vary *Upper row*: non-calcified raphe *Middle row*: Moderately calcified raphe *Lower row*: Severly calcified raphe	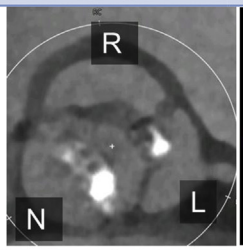 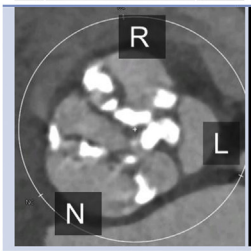 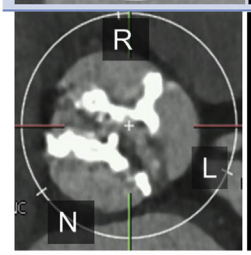	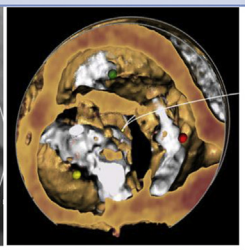 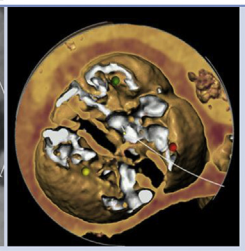 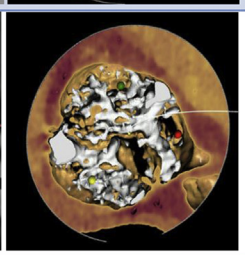	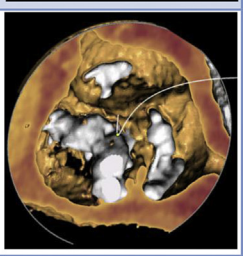 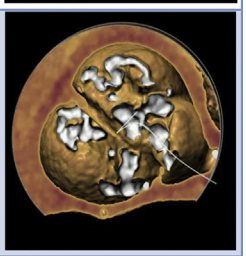 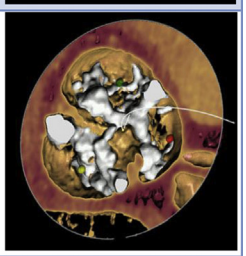
Acquired/ functional bicuspid valve (underlying tricuspid anatomy)	• Underlying tricuspid anatomy with symmetric Sinus of Valsalva • Non-opening commissure due to degenerative changes (here RL commissure) • Non-opening commissure reaches STJ, which is the distinguishing factor compared to a raphe	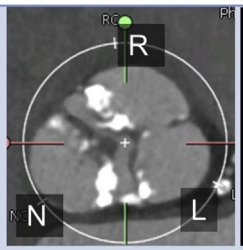	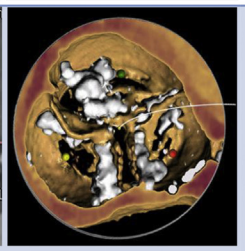	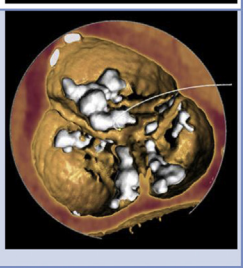

The STJ height should be measured in a perpendicular fashion to the annular plane using an electronic caliper tool from the annular plane to the lowest edge of the STJ, yielding a value in [mm] (Fig. 7). STJ diameter should be measured using a caliper tool on an imaging plane aligned with the STJ (Fig. 7).

3.8. ASCENDING AORTA. The ascending aorta should be assessed for the presence of aortopathy. Ascending aortic dimensions should be assessed on double-oblique multiplanar reformats in [mm] (Fig. 7).

3.9. OPTIMAL PROJECTION CURVE. Ideally, TAVI/TVAR is performed with fluoroscopic angulations providing a coplanar view of the aortic annulus without parallax. CT can be used to identify these patient-specific 'optimal' C-arm angulations (50,51). Use of these CT-derived angulations allows

Descargado para Anonymous User (n/a) en Consejeria de Sanidad de Castilla y Leon(Sacyl) de ClinicalKey.es por Elsevier en marzo 05, 2019.
Para uso personal exclusivamente. No se permiten otros usos sin autorización. Copyright ©2019. Elsevier Inc. Todos los derechos reservados.

FIGURE 6 **Identifying the Annular Plane in Bicuspid Aortic Valves With Sievers Type 0 Morphology**

Step & Description	Multi-planar reformats
Step 1: Start out with multi-planar images in default axial, sagittal, and coronal orientation; center cross-hairs onto the aortic valve	
Step 2: Align the cross-hairs in the sagittal and coronal views with the long axis of the aortic root; the resulting double oblique transverse view will depict the aortic valve en face.	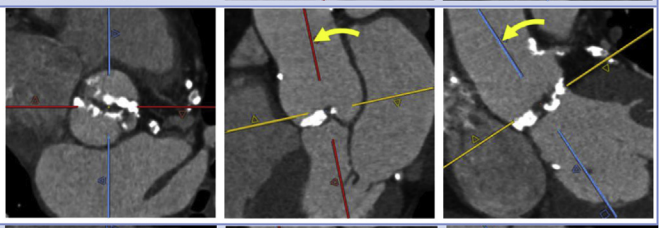
Step 3: Move the double oblique transverse plane up and down to identify the lowest insertion point of the more anterior/lateral cusp. Position the center of the cross-hairs exactly at the most basal insertion point (white arrow head).	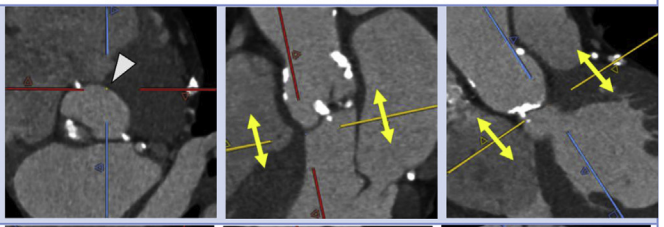
Step 4: Rotate the cross-hairs counter-clock-wise without moving up and down while maintaining its center position so that the formerly coronal view (here red cross-hair) transects the lowest insertion point of the medial/posterior cusp (white arrow head).	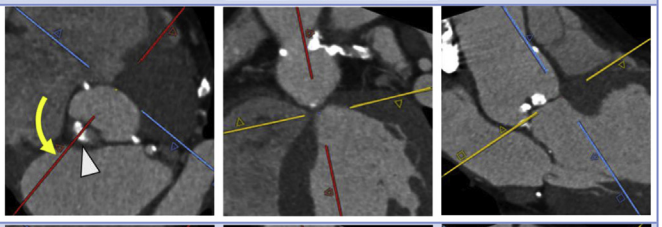
Step 5: The formerly coronal, now double-oblique view will show the lowest insertion points of both cusps (white arrows heads). In this view, rotate the (here orange) cross-hair indicating the double-oblique transverse view to transect exactly through the most basal insertion point of the medial/posterior cusp. Once this is achieved, the transverse double oblique plane will contain the most basal cusp insertion points of both cusps.	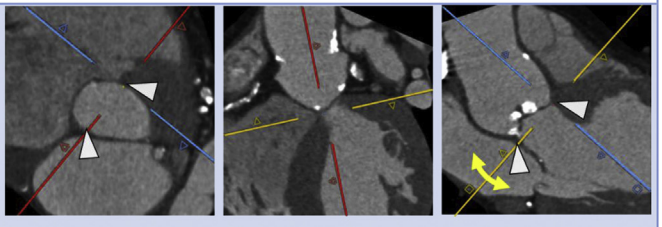
Step 6: Move the center of the cross-hairs to the center of the lumen (yellow arrow) without changing the orientation and position of the formerly coronal, now double-oblique view (red cross-hair). This is best done by scrolling through the formerly sagittal, now double oblique view.	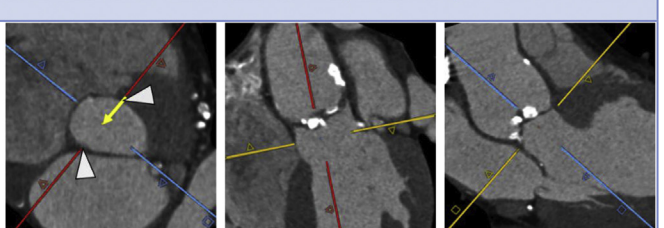
Step 7: In the formerly sagittal, now double oblique view, rotate the cross-hair of the transverse double oblique plane (here orange) while maintaining alignment with the most basal insertion points (arrow heads) until the smallest cross-sectional area is achieved on the transverse double oblique plane. **Over- and under-angulation results in overestimation of the annular cross-sectional area (dashed lines).**	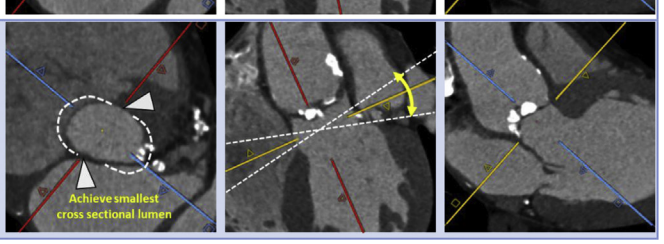

Descargado para Anonymous User (n/a) en Consejeria de Sanidad de Castilla y Leon(Sacyl) de ClinicalKey.es por Elsevier en marzo 05, 2019.
Para uso personal exclusivamente. No se permiten otros usos sin autorización. Copyright ©2019. Elsevier Inc. Todos los derechos reservados.

FIGURE 7 Schematic for Assessment of Aortic Root Dimensions

Item	Multiplanar reformats
Left Coronary Height The left coronary height is obtained by measuring with a caliper tool [mm] perpendicularly from the annular plane to the lower edge of the LCA ostium.	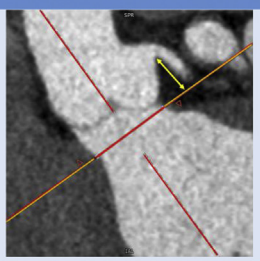
Right Coronary Height The right coronary height is obtained by measuring with a caliper tool [mm] perpendicularly from the annular plane to the lower edge of the RCA ostium	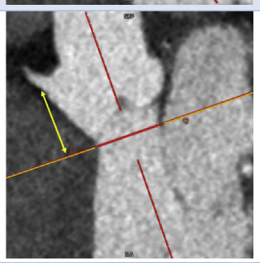
Sinotubular Junction Height The sinotubular junction height is obtained by measuring with a caliper tool [mm] perpendicularly from the annular plane to the lowest point of the sinotubular junction.	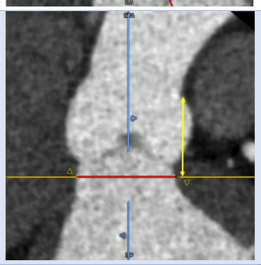
Sinus of Valsalva Diameter The sinus of Valsalva Diameter is assessed on a transverse double oblique plane at its widest dimensions with the plane commonly kept in parallel with the annular plane; three cusp to commissure distance measurements are taken; in case of symmetric dimensions, the final reported value is the average of these three [mm].	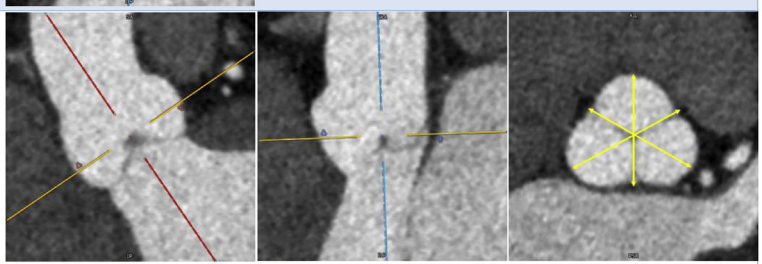
Sinotubular Diameter The sinotubular diameter is measured on a transverse, double oblique plane which is aligned with the sinotubular junction and commonly not parallel to the annular plane; a single diameter measurement [mm] is taken.	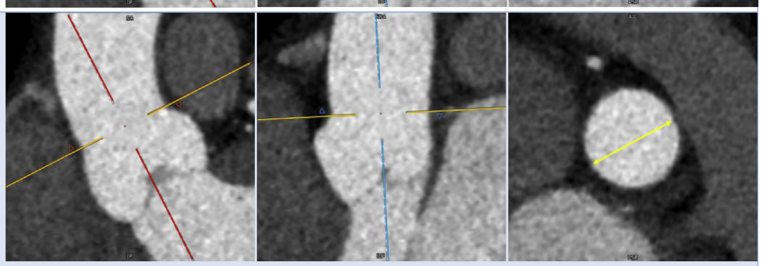
Ascending Aorta Diameter The ascending aorta diameter is measured on a transverse, double oblique plane which is oriented perpendicular to the long axis of the ascending aorta, either at the level of greatest width, or at the level of the main pulmonary artery (default); a single diameter measurement [mm] is taken.	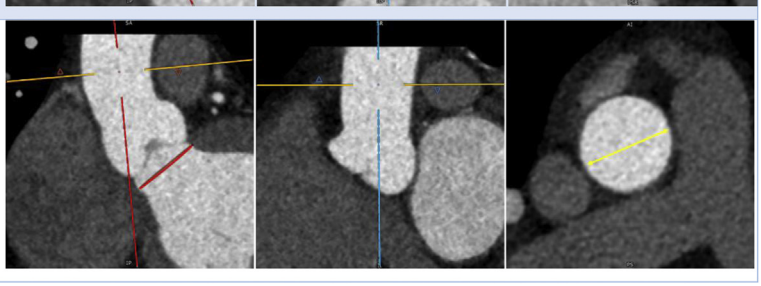

Descargado para Anonymous User (n/a) en Consejeria de Sanidad de Castilla y Leon(Sacyl) de ClinicalKey.es por Elsevier en marzo 05, 2019.
Para uso personal exclusivamente. No se permiten otros usos sin autorización. Copyright ©2019. Elsevier Inc. Todos los derechos reservados.

TABLE 6 Summary of Recommendations for the Reporting of Fluoroscopic Angulation

Recommendation	Grade of Recommendation*
Fluoroscopic planning	
Provision of optimal fluoroscopic projection angulations based on CT for each individual patient should be considered.	Strong
If the patient is not positioned supine for the CT examination, this should be noted in the report and proposed fluoroscopic angles should not be provided	Strong

*Based on level of consensus.
CT = computed tomography; TAVR = transcatheter aortic valve replacement.

optimization of initial pre-deployment fluoroscopic angulation, reducing the need for repeat pre-deployment root shots thereby reducing radiation exposure, contrast usage and procedural time (52,53). Optimal C-arm angulations should be reported as degrees [°] LAO or RAO with the corresponding values for cranial or caudal angulation. Dependent on institutional preferences, typically views are either centered on the right coronary cusp, or use predefined LAO angulation (e.g., LAO 10°), or are optimized for visualization of the left main stem. When identified projections result in cranial or caudal angulation >25°, alternate angulations should be provided, given the physical restraints of the C-arms. However, it is essential to recognize that CT predicted angulations are only valid if the patient's chest is positioned in a similar fashion on the CT table as during the procedure. Please refer to Table 6 for a summary of recommendations.

3.10. SIZING CONSIDERATIONS. CT is the non-invasive imaging gold standard for annular sizing and THV selection (1). In clinical practice, balloon expandable devices are largely sized on the basis of annular area, with self-expandable devices relying on perimeter. The reasons for this are partly historical but also reflect different risk profiles of these devices and the geometric implications of sizing with the different variables. Sizing based on manually assessed short and long axis diameters have been shown to be less reproducible (54), and can be considered obsolete.

3.10.1. Oversizing. The term 'oversizing' has been introduced over the last 6 years to help describe when a THV is deployed that is larger than the native annulus. The term 'oversizing' is a generic term as oversizing can be calculated based on any measurement of the annulus. In routine, oversizing is calculated as a percentage [%], as follows:

$$\text{Oversizing [\%]} = (\text{THV nominal measurement} / \text{annular measurement} - 1) \times 100$$

It is important to recognize, that the percentage oversizing calculated is strongly dependent on the annular measurement used, with very different implication of oversizing area than oversizing perimeter or perimeter derived diameter (55). Given the formula of a circle where area = π*radius^2 and circumference = π*diameter, the area increases exponentially while perimeter increases proportionally with increasing diameter. The percentage area oversizing is approximately 2-fold greater than the percentage perimeter when dealing with a perfect circle but the implications are even greater than expected owing to the non-circular geometry of the annulus. Both annular area and perimeter are clinically acceptable, but it is imperative that the imager and implanting physician appreciate the differences and are aware of the parameter being used for device sizing of specific devices. Further, the optimal threshold for oversizing is also device specific (56,57). Thus routine reporting of oversizing is not required, however familiarity of the concept is beneficial for subsequent discussion in Heart Team meetings.

3.10.2. Modification of sizing based on root calcification. CT not only provides information regarding annular size, but also provides important ancillary information that is helpful in guiding sizing and THV selection. Annular and sub-annular calcification, particularly when protruding into the lumen, can result in increased risk of both annular rupture and paravalvular regurgitation. Protruding landing zone calcification below the non-coronary cusp has been shown to be most closely-associated with annular injury, with this effect amplified when combined with aggressive annular oversizing (58). Presence, location and characteristics of subannular calcification should thus be integrated into all pre-TAVI/TAVR CT scan reports as described in the 'landing zone calcium' section.

3.10.3. Annular rupture. Annular rupture is an infrequent adverse event but is associated with a high mortality if it occurs (58,59). Patient and procedure related factors increasing risk of annular rupture include female sex, use of balloon-expandable valves, significant prosthesis oversizing, and prior radiation therapy. In addition, the presence of moderate/severe sub-annular calcification, particularly below the non-coronary cusp on pre-procedural CTA, is associated with a significantly increased risk for annular rupture (34). In addition, the depth of calcification within the LVOT is also important, as calcification immediately

Descargado para Anonymous User (n/a) en Consejeria de Sanidad de Castilla y Leon(Sacyl) de ClinicalKey.es por Elsevier en marzo 05, 2019.
Para uso personal exclusivamente. No se permiten otros usos sin autorización. Copyright ©2019. Elsevier Inc. Todos los derechos reservados.

TABLE 7 Summary of Recommendations for the Reporting of Vascular Access, Coronary Artery, and Non-Cardiac, Non-Vascular Findings

Recommendation	Grade of Recommendation*
Vascular access	
While facilitated or semi-automated work-flows may be used, the interpreter analyzing the imaging must be able to confirm the accuracy of the generated vessel centerline and perform manual corrections if required.	Strong
The minimal luminal diameter along both the right and left iliofemoral system should be provided including the anatomical location to the level of the expected puncture site	Strong
All areas of >270° calcification in the iliofemoral arteries should be reported	Strong
Calcification located anteriorly at the site of probable puncture should be reported.	Strong
The report should include a clear description of all vascular pathologies including aneurysms, dissection, and occlusions.	Strong
Coronary arteries	
Reporting of the coronary arteries for severity of coronary artery disease can be considered in appropriately selected patients, if image quality is of diagnostic quality	Strong
The presence and course of anomalous coronary arteries should be reported.	Strong
Non-cardiac, non-vascular	
CT images should be reviewed for incidental findings	Strong
Extracardiac findings should be reviewed and reported in the context of the healthcare environment and health status of the patient	Strong
Significant findings should be included in the dictated report and when appropriate verbally communicated to the Heart team.	Strong

*Based on level of consensus.

CT = computed tomography; SOV = sinus of valsalva; STJ = sinotubular junction; TAVI = transcatheter aortic valve implantation; TAVR = transcatheter aortic valve replacement.

below the annular plane connotes a higher risk than calcification lower within the LVOT. Protruding nodules of calcification are considered to connote higher risk than flat or mural calcification. The risk of aortic annulus rupture increases with the degree of oversizing of the prosthesis (particularly with >20% oversizing) and with the extent of calcification of the upper part of the LVOT (within 2 mm below the annulus plane) particularly when immediately below the non-coronary cusp (34,58).

3.10.4. Atrio-ventricular conduction block. An increased depth of implantation is the most frequently identified predictor of LBBB with both balloon- and self-expandable prostheses (60–65). Reduced implant depth during TAVI/TAVR has been shown to significantly decrease mortality and permanent pacemaker insertion rate (66). In addition, shorter length of the semi-membranous septum has been reported to be associated with higher risk of conduction disturbance post TAVI/TAVR, with a length of less than approx. 8mm predictive of high-degree AV-block, particularly when combined with a deep implant depth, or the presence of pre-existent right bundle branch block (41,42,67). The length of the semi-membranous septum can be measured in the coronal plane, at the longest point between the annular level and the muscular septum (67). However, routine assessment of semi-membranous septum length has not seen widespread adoption into clinical routine.

4. VASCULAR ACCESS

4.1. OVERVIEW. Vascular complications are independently associated with increased morbidity and mortality after TAVI/TAVR, however the rates of complications have fallen with improved pre-procedural screening with major vascular complications currently occurring in 4.5% of procedures (68,69). Access sheath sizes have reduced in size, however this simply shifts the threshold at which trans-femoral access can be achieved, rather than negating the importance of identification and quantification of vascular disease and dimensions (70). Given the continuous evolution of delivery systems, no reference is made to current devices and vessel diameter requirements. Please refer to **Table 7** for a summary of recommendations.

Analysis of iliofemoral vessel size, calcification, and tortuosity is required to determine if trans-femoral access can be achieved or whether an alternative access route is required (71,72). Due to its ability to accurately quantify all these aspects, CT provides greater predictive value for vascular complications than invasive angiography (73).

Risk factors for vascular complications are an external sheath diameter that exceeds the minimal artery diameter, moderate or severe calcification, and vessel tortuosity (75–77). While early reports described an increased risk at a sheath:diameter ratio ≥1.05, more recent work on modern access devices which are typically smaller with an increasing prevalence of expanding sheath designs, suggests a more liberal threshold of ≥1.12 can be safely used (73).

4.2. QUANTIFICATION OF LUMINAL DIMENSIONS. The minimal diameter of the vasculature between the aortic valve and the right and left common femoral

Descargado para Anonymous User (n/a) en Consejeria de Sanidad de Castilla y Leon(Sacyl) de ClinicalKey.es por Elsevier en marzo 05, 2019.
Para uso personal exclusivamente. No se permiten otros usos sin autorización. Copyright ©2019. Elsevier Inc. Todos los derechos reservados.

artery should be reported. This can be performed either manually on multiplanar reformats using a double-oblique technique, or using semi-automatic post-processing using centerline placement and curved multiplanar reformats. When the latter is used, manual verification of the center line should be performed to ensure accurate vessel tracking, and appropriate intra-luminal location of the centerline. When using either technique, attention should be paid to the potential for calcium blooming artifact, and appropriate windowing used to correct for this where necessary. It should also be ensured that all measurements are performed perpendicular to the long axis of the vessel at the location of the maximum stenosis. Transverse source images allow no more than a preliminary assessment of vessel size.

4.3. CALCIFICATION. Extend and distribution of calcifications of the iliofemoral vasculature should be assessed and reported. To describe the severity, a subjective, semi-quantitative grading scale can be used: none, mild (spotty), moderate (coalescing), severe (bulky, protruding, horse-shoe, circumferential). Care should be taken to identify circumferential or near-circumferential (horse-shoe) calcification particularly in areas of tortuosity or bifurcations, as these prevent vessel expansion when the sheath and valve passes through.

4.4. TORTUOSITY. Tortuosity of vascular structures can be assessed on transverse source images, but evaluation is facilitated using a volume rendered display from multiple viewing angles, such as anterior-posterior and RAO or LAO projections. In the absence of calcification, Iliofemoral arterial tortuosity is not necessarily a contraindication for femoral access, as tortuous vessel segments usually straightened with sheath insertion. However, when calcified, tortuous segments carry a substantial risk of access failure and the operator should be advised about this situation.

4.5. ACCESS SITE. Careful interrogation of the common femoral artery puncture site is important to ensure that that there is no focal stenosis nor calcifications anteriorly that may interfere with the arterial puncture or deployment of arterial closure devices (74). Also, the anatomy should be reviewed for the presence of a high femoral artery bifurcation. Relevant findings should be reported, ideally with detailed location in relation to fluoroscopically identifiable anatomical landmarks, such as the level of the femoral head (e.g., lower third).

4.6. AORTA. For transfemoral access, the thoracic and abdominal aorta should be assessed for the presences of relevant pathologies. In particular, the presence of ascending aortic aneurysm and the degree of ascending aortic calcification should be noted—the latter relevant for potential cross-clamping. Further relevant pathologies include abnormal elongation and kinking, dissections, aneurysms, and exophytic plaque.

4.7. ALTERNATE ACCESS. If transfemoral access is not feasible, depending on local practice, subclavian and/or carotid arteries can be reported using the same techniques and reporting parameters of the iliofemoral vessels (78,79). Due to more favorable angulation, an left-sided approach is preferred for subclavian access. Finally, if a transcaval approach is to be considered, the presence, size and level of calcification free windows of the aortic wall adjacent to the inferior vena cava should be reported (80). Additionally the report should also include a clear description of all vascular pathologies including aneurysms, dissection, and occlusions.

5. CORONARY ARTERIES

In the setting of good image quality, modest motion artifact in particular, coronary CTA can rule out significant coronary stenosis with high negative predictive value (81–85). However confident assessment of coronary stenosis severity on TAVI/TAVR scans is challenging, particularly due to a high prevalence of coronary calcification and higher heart rates resulting in motion artifact (86). Beta-blockade must be used with caution and nitroglycerin is contra-indicated, with the absence of these associated with reduced diagnostic accuracy (9). Independent from the assessment for CAD, the presence and course of anomalous coronary arteries, easily interpreted, should be reported.

6. INCIDENTAL NON-CARDIAC NON-VASCULAR FINDINGS

With growing evidence and increasing clinical adoption, TAVI/TAVR is increasingly being performed in younger patients with lower risk profiles. This increases the relevance of incidental findings on CT as the life expectancy of patients undergoing TAVI/TAVR will be longer than in the past. All imaging obtained should be reviewed carefully for incidental findings. This is best performed by trained radiologists, either as a combined or separate report according to local practices. The clinical recommendations and downstream management of incidental findings on pre-TAVI/TAVR CT will vary according to the risk profile and life expectancy of the patients as well as local clinical practice. Please refer to **Table 7** for a summary of recommendations.

Descargado para Anonymous User (n/a) en Consejeria de Sanidad de Castilla y Leon(Sacyl) de ClinicalKey.es por Elsevier en marzo 05, 2019.
Para uso personal exclusivamente. No se permiten otros usos sin autorización. Copyright ©2019. Elsevier Inc. Todos los derechos reservados.

FIGURE 8 MPR Alignment and Semi-Quantitative Grading of Hypo-Attenuated Leaflet Thickening

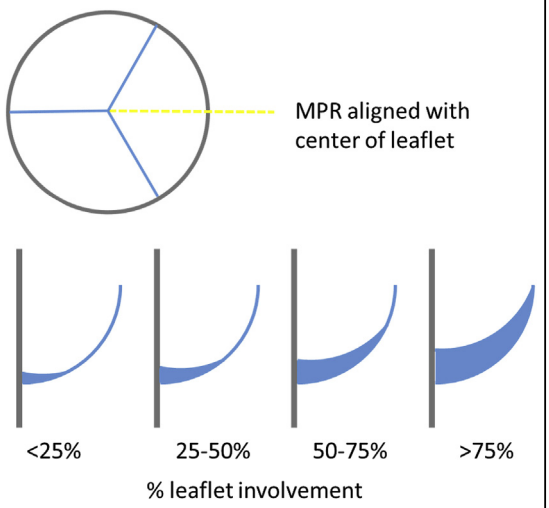

The **dashed yellow line** indicates the orientation of the long axis views in the **lower row**, aligned with the center of the cusps. The extent of leaflet thickening can be graded on a subjective 4-tier grading scale along the curvilinear orientation of the leaflet. Typically, hypo-attenuated leaflet thickening appears meniscal-shaped on long axis reformats, with greater thickness at the base than towards the center of the leaflet.

7. POST-TAVI/TAVR CT

Echocardiography is the test for evaluation of transcatheter heart valve function and durability (87,88). CT enables post-implant imaging of transcatheter heart valves (geometry, position, leaflets) (89-98), There is however, no consensus regarding the clinical need to perform routine cardiac CT in TAVI/TAVR recipients. Cardiac CT is an important adjunctive modality to echocardiography in patients where there is concern for valve thrombosis, infective endocarditis, or structural degeneration (24,99). Hypoattenuated leaflet thickening (HALT) (**Figs. 8 and 9**) and restricted leaflet motion (also referred to as HAM [hypoattenuation affecting motion]) determined by CT often indicate leaflet thrombus formation (7,8,100-102). When echocardiography is indeterminate, CTA can be useful for adjudication of leaflet thrombus. When imaging in the post TAVI/TAVR setting for the assessment of HALT, full cardiac cycle imaging is recommended to maximize image quality and to permit assessment of leaflet motion. IV contrast administration and timing should be performed as per the routine TAVI/TAVR workup, although a smaller contrast dose is required due to the lack of need for peripheral vasculature imaging. Leaflet thickening should be described based on location, extent in length and overall thickness. Importantly, HALT takes a meniscal shape when viewed on a long-axis MPR at the center of the cusp (**Figs. 8 and 9**). In regard to extent of HALT along the curvilinear leaflet, as subjective grading scale can be employed as outlined in **Figure 8**.

Restricted motion should be reported as present or absent. Restricted valve motion without thickening on CTA is rare and should be reported with great caution, to avoid the risk of unnecessary treatment (100,102,103).

8. VALVE-IN-VALVE IMPLANTATION

8.1. OVERVIEW. Valve in valve (VIV) implantation of THVs into failing bioprosthetic valves has evolved as a treatment alternative with high technical success rates and promising patient outcomes (104). Broadly, bioprosthetic valves can be categorized as stented surgical (rigid scaffold), stentless surgical (no rigid scaffold), and transcatheter heart valves.

The Valve-in-Valve International Data (VIVID) Registry has shown that coronary occlusion is more common in VIV than TAVI/TAVR in native aortic stenosis, with occlusion reported in 2.3% of VIV compared with 0.66% in native valve TAVI/TAVR (48,105). Factors related to the observed higher frequency are canted position of the stented surgical bioprosthesis within the aortic root and small root dimensions, the latter in particular in patients with stentless surgical valves. Pre-procedural CT plays a limited role in THV sizing, but a key role in the discrimination of patient specific risk for coronary occlusion. Vascular access should be reported as for TAVI/TAVR in native aortic valves (see Vascular Access section). Please refer to **Table 8** for a summary of recommendations.

8.2. ASSESSMENT FOR RISK OF CORONARY ARTERY OBSTRUCTION. Implantation of a THV within a stented surgical valve is technically different from TAVR in native aortic valves, as the stented bioprosthetic valves provides the scaffold for THV anchorage. The THV displaces the bioprosthetic leaflets into an open position with the THV frame and overlying bioprosthetic leaflets forming a ‘covered’ cylinder. The anatomical orientation of the cylinder is being dictated by the orientation of the surgical valve. Frequently, the surgical valve is implanted in a canted fashion in regard to the long axis of the aortic root, with the potential for close proximity of the bioprosthetic leaflets/THV to the coronary ostia and

Descargado para Anonymous User (n/a) en Consejeria de Sanidad de Castilla y Leon(Sacyl) de ClinicalKey.es por Elsevier en marzo 05, 2019.
Para uso personal exclusivamente. No se permiten otros usos sin autorización. Copyright ©2019. Elsevier Inc. Todos los derechos reservados.

FIGURE 9 **Examples of Hypo-Attenuated Leaflet Thickening in Both Self-Expandable (Upper Row) and Balloon-Expandable Device (Lower Row) With Varying Degree of Thickening: Limited to Base, i.e., <25% Leaflet Involvement (Left Column) and Near Complete Leaflet Involvement, i.e., >75% (Right Column)**

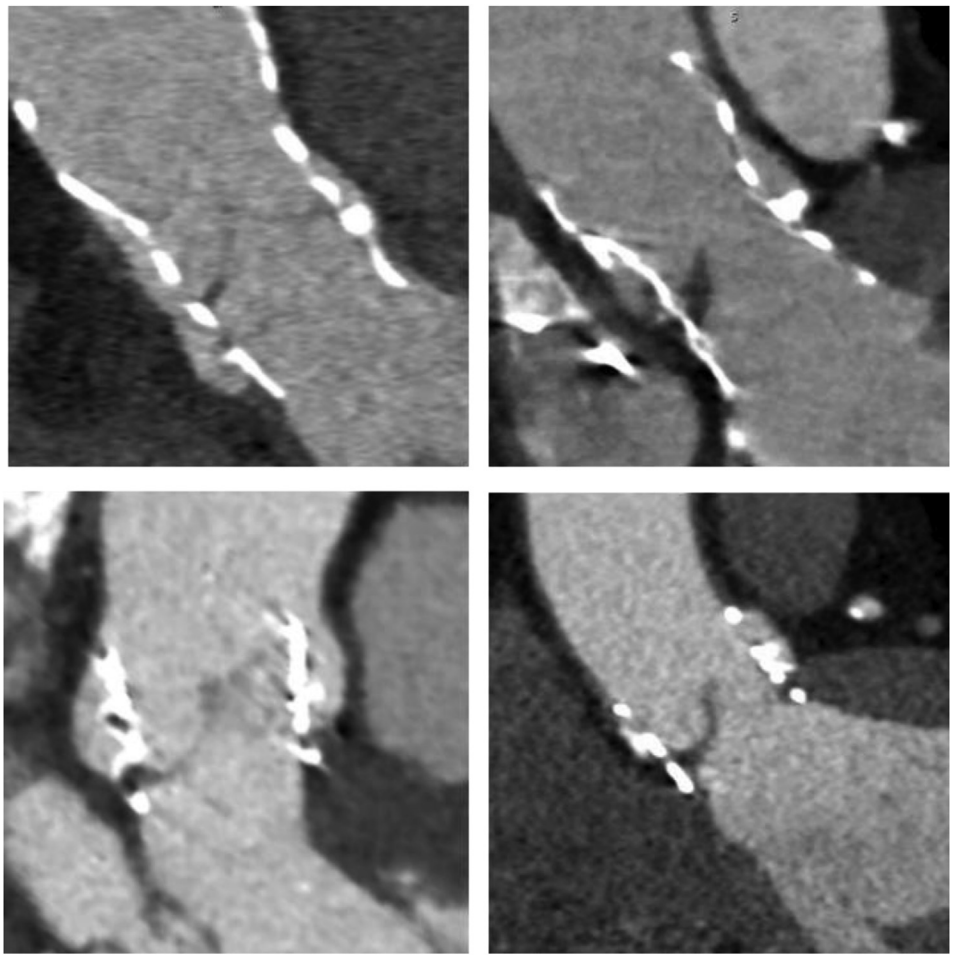

TABLE 8 **Summary of Recommendations for the Reporting of Post TAVI/TAVR and Pre-VIV Scans**

Recommendation	Grade of Recommendation*
Post TAVR	
At present, routine CT imaging following TAVI/TAVR is not recommended	Strong
CT should be considered in the setting of clinical concern for valve thrombosis, infective endocarditis, or structural valve degeneration	Strong
Leaflet thickening should be described based on location, extent in length and overall thickness	Strong
Restricted motion should be reported as present or absent	Strong
Valve-in-valve	
When available the size of the surgical valve in situ should be obtained from the patient records. When this is not possible, internal diameter may be measured and used for calculating the valve to be inserted	Strong
The relationship of the uppermost aspect of the surgical valve struts to the STJ and to the coronaries should be described	Strong
When the surgical valve struts end below the level of the coronary ostia, virtual transcatheter valve to coronary ostia distances do not need to be measured.	Strong
Stentless surgical valve in valve procedures should be interpreted and reported as for native TAVI/TAVR cases regarding risk of coronary occlusion	Strong

*Based on level of consensus.

CT = computed tomography; SOV = sinus of valsalva; STJ = sinotubular junction; TAVI = transcatheter aortic valve implantation; TAVR = transcatheter aortic valve replacement.

Descargado para Anonymous User (n/a) en Consejeria de Sanidad de Castilla y Leon(Sacyl) de ClinicalKey.es por Elsevier en marzo 05, 2019.
Para uso personal exclusivamente. No se permiten otros usos sin autorización. Copyright ©2019. Elsevier Inc. Todos los derechos reservados.

FIGURE 10 Workflow for Assessment of Coronary Obstruction Risk in Patients Undergoing Transcatheter Valve-in-Valve Procedure

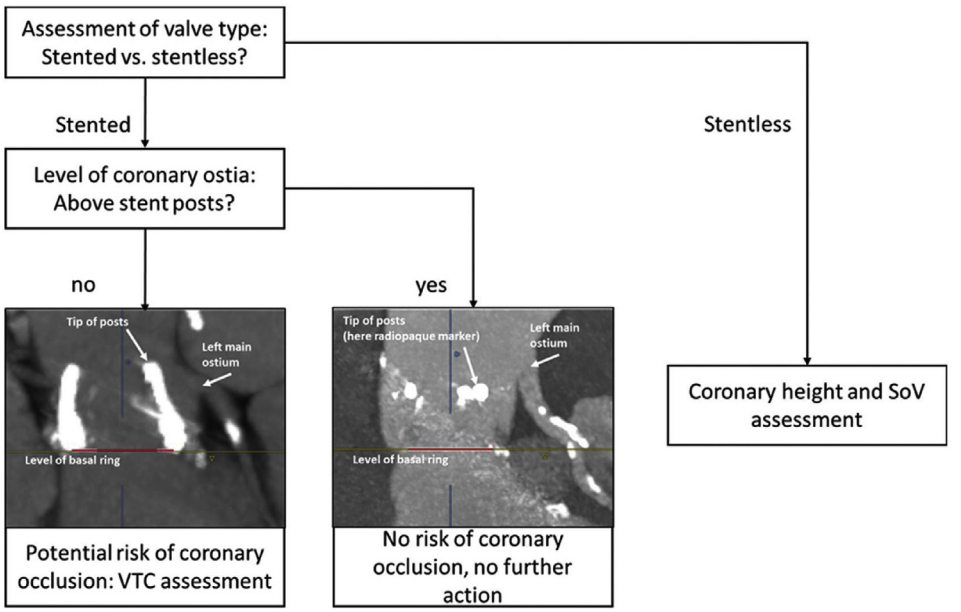

Virtual THV to coronary (VTC) distance should be assessed in patients with stented valves and coronary artery orifices originating at the level of the prosthetic heart valve.

subsequent risk of coronary obstruction despite a large aortic root. Conceivably, the distortion is not adequately described by the coronary artery height and sinus of Valsalva width. To account for this anatomical distortion, the concept of predicting the distance from the anticipated, expanded THV frame to the coronary artery orifice, also referred to as the virtual THV to coronary (VTC) distance was introduced (106). This concept was validated in a recent VIVID multicenter analysis, which demonstrated the VTC to be the only independent predictor of coronary obstruction, with a VTC of less than 4 mm indicating an increased risk of coronary artery obstruction (105).

It is recommended that the VTC is assessed for the right coronary artery and the left main coronary artery, if the posts extend to or above the level of the orifices (**Fig. 10**). If the coronary arteries originate above the posts, obviously no VTC is required.

The VTC can be assessed using either a multiplanar reformat (MPR) capable of producing a circular region of interest (ROI), or an advanced post-processing platform capable of simulating a virtual cylinder with a defined diameter and height (106) (**Fig. 11**). The MPRs should be carefully aligned with the orientation of the surgical valve. The ROI is drawn at the level of the coronary artery orifice and the distance from the ROI to the orifices is assessed with a caliper tool and reported in [mm]. Dependent on the configuration of the aortic root, the sinus wall or STJ can come into closer proximity to the expanded THV above the ostium. For this reason, VTC assessment should not be confined to the level of the ostium but additional measurements should be employed above the ostium to identify the risk of potential sealing.

Sinus of Valsalva (SOV) width and coronary ostia height can also be measured but the VTC has been shown to provide incremental risk discrimination as the other measurements do not take into account the SHV tilting/canting. VTC distances <4mm should be highlighted as being at high risk of procedure related coronary obstruction (105).

Implantation of a THV within a stentless surgical valve is biomechanically similar to TAVR in native stenosis due to the absence of a rigid scaffold. However, stentless surgical valves are often employed in small root anatomies. This, in combination with anatomical distortion increases the risk of coronary obstruction. Stentless surgical valve cases should be interpreted similar to native aortic stenosis cases regarding risk of coronary occlusion, with the sinus dimensions and coronary heights measured and reported as described earlier.

8.3. THV SIZING. If unknown, the size of a SAVR can be estimated from measuring the internal area of the basal SAVR ring on the CT reconstructions and

Descargado para Anonymous User (n/a) en Consejeria de Sanidad de Castilla y Leon(Sacyl) de ClinicalKey.es por Elsevier en marzo 05, 2019.
Para uso personal exclusivamente. No se permiten otros usos sin autorización. Copyright ©2019. Elsevier Inc. Todos los derechos reservados.

FIGURE 11 Pre-Procedural Assessment of Virtual THV to Coronary Artery Distance in Patients Undergoing Transcatheter Valve-in-Valve Procedure

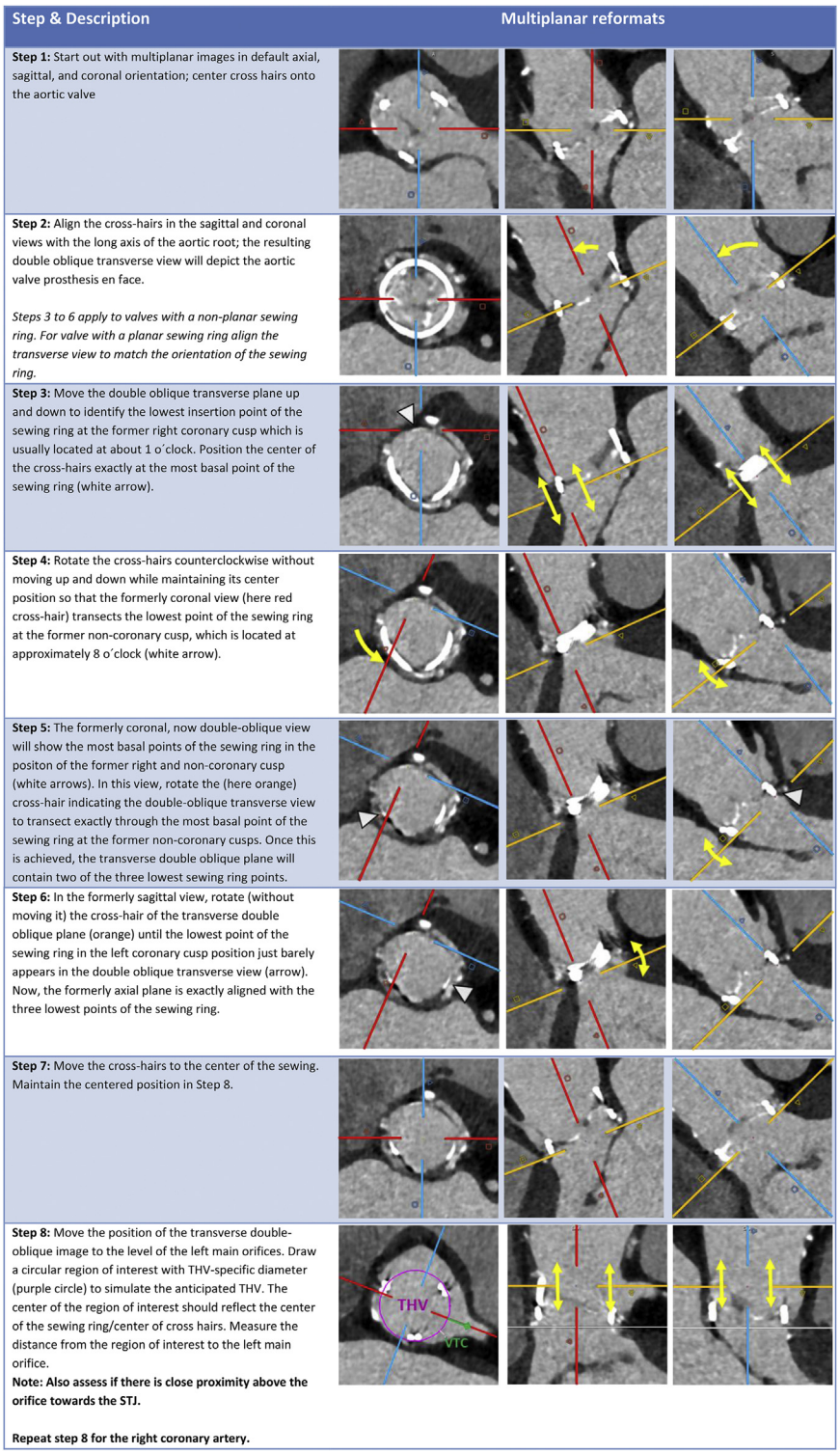

The example shown here features a stented valve with a non-planar basal sewing ring. Steps 3 to 6 account for identifying alignment with the three most basal points. In case of a planar basal ring, these steps can be omitted.

Descargado para Anonymous User (n/a) en Consejeria de Sanidad de Castilla y Leon(Sacyl) de ClinicalKey.es por Elsevier en marzo 05, 2019.
Para uso personal exclusivamente. No se permiten otros usos sin autorización. Copyright ©2019. Elsevier Inc. Todos los derechos reservados.

cross-referencing with published reference charts (107,108). However, reference charts are currently limited to two publications and do not reflect the complete complement of available SAVRs, with different measurement techniques used in both of these. When using reference charts careful adherence to the measurement technique employed in the respective papers is required to allow for accurate estimation of the valve size.

8.4. REQUIREMENTS FOR CT DATA ACQUISITION AND RECONSTRUCTION. As anatomical information of both the aortic root and aorto/ilio/femoral vasculature is required pre-VIV, the requirements for CT data acquisition and reconstruction are similar to those for planning of TAVR in native aortic valve. The contrast-enhanced, ECG-synchronized cardiac CT acquisition should cover at least the aortic root. In stented surgical valves, the lack of dynamism due to the rigid bioprosthetic heart valve scaffold requires only a single ECG-synchronized frame. However, acquisition and reconstruction of the entire cardiac cycle allows for additional CT data which may be beneficial in case of motion or misregistration artifacts. Of note, in the setting of stented surgical valves with radiopaque scaffolds, a non-contrast CT dataset may be sufficient for assessment of coronary obstruction risk, as coronary artery orifices can be identified based on surrounding epicardial fatty tissue. In patients with stentless surgical valves, acquisition protocols for native aortic stenosis should be employed, and contrast enhancement is required.

9. REPORTING

All measurements of the aortic root and access route should to be stored as screenshots in the picture archiving and communication system (PACS) for future review and reference. Screenshots should ideally include MPR reference images with crosshairs displayed, which allows to comprehend the orientation and location of the imaging plane on which the measurement was taken. Pertinent components of a comprehensive report are listed in Table 9.

TABLE 9 Pertinent Components of a Comprehensive Pre-TAVR/TAVI CT Report

Category	Items
Aortic root findings	1 Valve morphology [tricuspid, congenital bicuspid according to e.g., Sievers classification, functional/acquired bicuspid] 2 Calcium distribution [symmetric, asymmetric, bulky, bulky at free edge] 3 Aortic annular dimension a Overall image quality [good, fair, poor] b When assessed (systole/diastole, reconstruction phase) c Annular area [mm^2] d Annular perimeter [mm] e Optional min and max diameter [mm] 4 Presence of annular and subannular calcification a Extent [crescent non-protruding vs. bulky protruding, intramural] b Location 5 LM height [mm] 6 RCA height [mm] 7 SoV averaged [mm] 8 STJ [mm], report if calcified 9 Optimal coplanar projection [LAO/RAO and corresponding CRA/CAU angulation]
Aorto/ilio/femoral vasculature	1 Pathologies of the ascending aorta 2 Pathologies of the aortic arch, descending thoracic/abdominal aorta 3 Iliofemoral vasculature a Minimal diameters with location b Extent [mild, moderate, severe] and location of calcification/plaque; particular emphasis on horse-shoe, circumferential pattern c Tortuosity 4 Common femoral artery access site a Calcium (posterior, anterior; anterior has implication for closure system) b Report findings in regard to the level of the femoral head (upper third, center, lower third) c Level of femoral bifurcation if at level of femoral head
	1 Subclavian artery a Minimal diameter b Calcification, in particular at ostium c Tortuosity 2 Other access approaches such as trans-aortic, trans-carotid or trans-caval depending on site preferences
Other cardiac findings	Report relevant cardiac findings, such as chamber size, myocardial scar, evidence of other valvulopathies including MAC
Other findings	Report relevant extra-cardiac pathologies and relevant incidental findings
Impression	1 Valve morphology, annular area, relevant root features (e.g., adverse root features such as calcification, low coronary artery height, non-spacious sinus of Valsalva) 2 Comment on feasibility of trans-femoral access; adverse features such as horse-shoe/circumferential calcium, severe tortuosity, anterior common femoral artery calcium 3 Relevant incidental findings.

10. SUMMARY

CT imaging plays an important role in procedural planning for TAVI/TAVR and should be a fully integrated component of any TAVI/TAVR program. The use of CT in TAVI/TAVR is multifaceted and should include appropriate image acquisition and reconstruction as well as the comprehensive assessment the aortic root and vascular access. Importantly, the individuals responsible for the interpretation of the CT examination should be part of the Heart team to ensure appropriate incorporation of the data from the CTA into the patient selection process and procedure planning.

ADDRESS FOR CORRESPONDENCE: Dr. Philipp Blanke, St. Paul's Hospital and University of British Columbia, Radiology, 1081 Burrard Street, Vancouver, BC V1Z 1Y6, Canada. E-mail: phil.blanke@gmail.com.

Descargado para Anonymous User (n/a) en Consejeria de Sanidad de Castilla y Leon(Sacyl) de ClinicalKey.es por Elsevier en marzo 05, 2019.
Para uso personal exclusivamente. No se permiten otros usos sin autorización. Copyright ©2019. Elsevier Inc. Todos los derechos reservados.

REFERENCES

1. Achenbach S, Delgado V, Hausleiter J, Schoenhagen P, Min JK, Leipsic JA. SCCT expert consensus document on computed tomography imaging before transcatheter aortic valve implantation (TAVI)/transcatheter aortic valve replacement (TAVR). J Cardiovasc Comput Tomogr 2012; 6:366–80.

2. Leon MB, Smith CR, Mack M, et al. Transcatheter aortic-valve implantation for aortic stenosis in patients who cannot undergo surgery. N Engl J Med 2010;363:1597–607.

3. Kapadia SR, Leon MB, Makkar RR, et al. 5-year outcomes of transcatheter aortic valve replacement compared with standard treatment for patients with inoperable aortic stenosis (PARTNER 1): a randomised controlled trial. Lancet 2015;385: 2485–91.

4. Mack MJ, Leon MB, Smith CR, et al. 5-year outcomes of transcatheter aortic valve replacement or surgical aortic valve replacement for high surgical risk patients with aortic stenosis (PARTNER 1): a randomised controlled trial. Lancet 2015; 385:2477–84.

5. Leon MB, Smith CR, Mack MJ, et al. Transcatheter or surgical aortic-valve replacement in intermediate-risk patients. N Engl J Med 2016;374:1609–20.

6. Reardon MJ, Van Mieghem NM, Popma JJ, et al. Surgical or transcatheter aortic-valve replacement in intermediate-risk patients. N Engl J Med 2017;376:1321–31.

7. Leetmaa T, Hansson NC, Leipsic J, et al. Early aortic transcatheter heart valve thrombosis: diagnostic value of contrast-enhanced multidetector computed tomography. Circ Cardiovasc Interv 2015;8:1–9.

8. Pache G, Schoechlin S, Blanke P, et al. Early hypo-attenuated leaflet thickening in balloon-expandable transcatheter aortic heart valves. Eur Heart J 2016;37:2263–71.

9. Abbara S, Blanke P, Maroules CD, et al. SCCT guidelines for the performance and acquisition of coronary computed tomographic angiography: a report of the society of cardiovascular computed tomography guidelines committee: endorsed by the north American society for cardiovascular imaging (NASCI). J Cardiovasc Comput Tomogr 2016; 10:435–49.

10. Suchá D, Tuncay V, Prakken NHJ, et al. Does the aortic annulus undergo conformational change throughout the cardiac cycle? A systematic review. Eur Heart J Cardiovasc Imaging 2015;16:1307–17.

11. Jurencak T, Turek J, Kietselaer BLJH, et al. MDCT evaluation of aortic root and aortic valve prior to TAVI. What is the optimal imaging time point in the cardiac cycle? Eur Radiol 2015;25: 1975–83.

12. Willson AB, Webb JG, Freeman M, et al. Computed tomography-based sizing recommendations for transcatheter aortic valve replacement with balloon-expandable valves: comparison with transesophageal echocardiography and rationale for implementation in a prospective trial. J Cardiovasc Comput Tomogr 2012;6:406–14.

13. De Heer LM, Budde RPJ, Van Prehn J, et al. Pulsatile distention of the nondiseased and stenotic aortic valve annulus: analysis with electrocardiogram-gated computed tomography. Ann Thorac Surg 2012;93:516–22.

14. Lewis MA, Pascoal A, Keevil SF, Lewis CA. Selecting a CT scanner for cardiac imaging: the heart of the matter. Br J Radiol 2016;89: 20160376.

15. Mylotte D, Sudre A, Teiger E, et al. Transcarotid transcatheter aortic valve replacement feasibility and safety. J Am Coll Cardiol Intv 2016; 9:472–80.

16. Søndergaard L, Steinbrüchel DA, Ihlemann N, et al. Two-year outcomes in patients with severe aortic valve stenosis randomized to transcatheter versus surgical aortic valve replacement: the all-comers nordic aortic valve intervention randomized clinical trial. Circ Cardiovasc Interv 2016;9: 1–10.

17. Tamburino C, Barbanti M, D'Errigo P, et al. 1-year outcomes after transfemoral transcatheter or surgical aortic valve replacement: results from the Italian OBSERVANT study. J Am Coll Cardiol 2015;66:804–12.

18. Spagnolo P, Giglio M, Di Marco D, et al. Feasibility of ultra-low contrast 64-slice computed tomography angiography before transcatheter aortic valve implantation: a real-world experience. Eur Heart J Cardiovasc Imaging 2016; 17:24–33.

19. Pulerwitz TC, Khalique OK, Nazif TN, et al. Very low intravenous contrast volume protocol for computed tomography angiography providing comprehensive cardiac and vascular assessment prior to transcatheter aortic valve replacement in patients with chronic kidney disease. J Cardiovasc Comput Tomogr 2016;10:316–21.

20. Bittner DO, Arnold M, Klinghammer L, et al. Contrast volume reduction using third generation dual source computed tomography for the evaluation of patients prior to transcatheter aortic valve implantation. Eur Radiol 2016;26:4497–504.

21. Nijssen EC, Rennenberg RJ, Nelemans PJ, et al. Prophylactic hydration to protect renal function from intravascular iodinated contrast material in patients at high risk of contrast-induced nephropathy (AMACING): a prospective, randomised, phase 3, controlled, open-label, non-inferiority trial. Lancet (London, England) 2017;389:1312–22.

22. Su X, Xie X, Liu L, et al. Comparative effectiveness of 12 treatment strategies for preventing contrast-induced acute kidney injury: a systematic review and bayesian network meta-analysis. Am J Kidney Dis 2017;69:69–77.

23. Clavel MA, Messika-Zeitoun D, Pibarot P, et al. The complex nature of discordant severe calcified aortic valve disease grading: new insights from combined Doppler echocardiographic and computed tomographic study. J Am Coll Cardiol 2013;62:2329–38.

24. Baumgartner H, Falk V, Bax JJ, et al. ESC/EACTS guidelines for the management of valvular heart disease: the task force for the management of valvular heart disease of the european society of cardiology (ESC) and the european association for cardio-thoracic surgery (EACTS). Eur Heart J 2017;2017:1–53.

25. Pawade T, Clavel M-A, Tribouilloy C, et al. Computed tomography aortic valve calcium scoring in patients with aortic stenosis. Circ Cardiovasc Imaging 2018;11:e007146.

26. Agatston AS, Janowitz WR, Hildner FJ, Zusmer NR, Viamonte M, Detrano R. Quantification of coronary artery calcium using ultrafast computed tomography. J Am Coll Cardiol 1990;15: 827–32.

27. Hecht HS, Blaha MJ, Kazerooni EA, et al. CAC-DRS: coronary artery calcium data and reporting system. An expert consensus document of the society of cardiovascular computed tomography (SCCT). J Cardiovasc Comput Tomogr 2018;12: 185–91.

28. Boehm T, Husmann L, Leschka S, Desbiolles L, Marincek B, Alkadhi H. Image quality of the aortic and mitral valve with CT:. Relative versus absolute delay reconstruction. Acad Radiol 2007;14: 613–24.

29. Suh YJ, Im DJ, Hong YJ, et al. Absolute-delay multiphase reconstruction reduces prosthetic valve-related and atrial fibrillation-related artifacts at cardiac CT. Am J Roentgenol 2017;208: W160–7.

30. Piazza N, de Jaegere P, Schultz C, Becker AE, Serruys PW, Anderson RH. Anatomy of the aortic valvar complex and its implications for transcatheter implantation of the aortic valve. Circ Cardiovasc Interv 2008;1:74–81.

31. Anderson RH. Clinical anatomy of the aortic root. Heart 2000;84:670–3.

32. Murphy DT, Blanke P, Alaamri S, et al. Dynamism of the aortic annulus: effect of diastolic versus systolic CT annular measurements on device selection in transcatheter aortic valve replacement (TAVR). J Am Coll Cardiol Intv 2016; 10:37–43.

33. Blanke P, Russe M, Leipsic J, et al. Conformational pulsatile changes of the aortic annulus: impact on prosthesis sizing by computed tomography for transcatheter aortic valve replacement. J Am Coll Cardiol Intv 2012;5:984–94.

34. Hansson NC, Nørgaard BL, Barbanti M, et al. The impact of calcium volume and distribution in aortic root injury related to balloon-expandable transcatheter aortic valve replacement. J Cardiovasc Comput Tomogr 2015;9:382–92.

35. Latsios G, Gerckens U, Buellesfeld L, et al. "Device landing zone" calcification, assessed by MSCT, as a predictive factor for pacemaker implantation after TAVI. Cathet Cardiovasc Interv 2010;76:431–9.

36. Ewe SH, Ng ACT, Schuijf JD, et al. Location and severity of aortic valve calcium and implications for aortic regurgitation after transcatheter aortic valve implantation. Am J Cardiol 2011;108:1470–7.

37. Jilaihawi H, Makkar RR, Kashif M, et al. A revised methodology for aortic-valvar complex calcium quantification for transcatheter aortic

Descargado para Anonymous User (n/a) en Consejeria de Sanidad de Castilla y Leon(Sacyl) de ClinicalKey.es por Elsevier en marzo 05, 2019.
Para uso personal exclusivamente. No se permiten otros usos sin autorización. Copyright ©2019. Elsevier Inc. Todos los derechos reservados.

valve implantation. Eur Heart J Cardiovasc Imaging 2014;15:1324–32.

38. Khalique OK, Hahn RT, Gada H, et al. Quantity and location of aortic valve complex calcification predicts severity and location of paravalvular regurgitation and frequency of post-dilation after balloon-expandable transcatheter aortic valve replacement. J Am Coll Cardiol Intv 2014;7:885–94.

39. Abramowitz Y, Jilaihawi H, Chakravarty T, et al. Balloon-expandable transcatheter aortic valve replacement in patients with extreme aortic valve calcification. Cathet Cardiovasc Interv 2016;87:1173–9.

40. Hansson NC, Leipsic J, Pugliese F, et al. Aortic valve and left ventricular outflow tract calcium volume and distribution in transcatheter aortic valve replacement: influence on the risk of significant paravalvular regurgitation. J Cardiovasc Comput Tomogr 2018;12:290–7.

41. Fujita B, Kütting M, Seiffert M, et al. Calcium distribution patterns of the aortic valve as a risk factor for the need of permanent pacemaker implantation after transcatheter aortic valve implantation. Eur Hear J Cardiovasc Imaging 2016;17:1385–93.

42. Maeno Y, Abramowitz Y, Kawamori H, et al. A highly predictive risk model for pacemaker implantation after TAVR. JACC Cardiovasc Imaging 2017;10:1139–47.

43. Mack MJ, Brennan JM, Brindis R, et al. Outcomes following transcatheter aortic valve replacement in the United States. JAMA, J Am Med Assoc 2013;310:2069–77.

44. Yoon S-H, Bleiziffer S, De Backer O, et al. Outcomes in transcatheter aortic valve replacement for bicuspid versus tricuspid aortic valve stenosis. J Am Coll Cardiol 2017;69:2579–89.

45. Sievers HH, Schmidtke C. A classification system for the bicuspid aortic valve from 304 surgical specimens. J Thorac Cardiovasc Surg 2007;133:1226–33.

46. Michelena HI, Prakash SK, Corte A Della, et al. Bicuspid aortic valve identifying knowledge gaps and rising to the challenge from the international bicuspid aortic valve consortium (BAVCON). Circulation 2014;129:2691–704.

47. Jilaihawi H, Chen M, Webb J, et al. A bicuspid aortic valve imaging classification for the TAVR era. J Am Coll Cardiol Img 2016;9:1145–58.

48. Ribeiro HB, Webb JG, Makkar RR, et al. Predictive factors, management, and clinical outcomes of coronary obstruction following transcatheter aortic valve implantation: insights from a large multicenter registry. J Am Coll Cardiol 2013;62:1552–62.

49. Ribeiro HB, Nombela-Franco L, Urena M, et al. Coronary obstruction following transcatheter aortic valve implantation: a systematic review. J Am Coll Cardiol Intv 2013;6:452–61.

50. Binder RK, Leipsic J, Wood D, et al. Prediction of optimal deployment projection for transcatheter aortic valve replacement: angiographic 3-dimensional reconstruction of the aortic root versus multidetector computed tomography. Circ Cardiovasc Interv 2012;5:247–52.

51. Gurvitch R, Wood DA, Leipsic J, et al. Multislice computed tomography for prediction of optimal angiographic deployment projections during transcatheter aortic valve implantation. J Am Coll Cardiol Intv 2010;3:1157–65.

52. Samim M, Stella PR, Agostoni P, et al. Automated 3D analysis of pre-procedural MDCT to predict annulus plane angulation and C-arm positioning: benefit on procedural outcome in patients referred for TAVR. J Am Coll Cardiol Img 2013;6:238–48.

53. Hell MM, Biburger L, Marwan M, et al. Prediction of fluoroscopic angulations for transcatheter aortic valve implantation by CT angiography: influence on procedural parameters. Eur Heart J Cardiovasc Imaging 2017;18:906–14.

54. Gurvitch R, Webb JG, Yuan R, et al. Aortic annulus diameter determination by multidetector computed tomography: reproducibility, applicability, and implications for transcatheter aortic valve implantation. J Am Coll Cardiol Intv 2011;4:1235–45.

55. Blanke P, Willson AB, Webb JG, et al. Oversizing in transcatheter aortic valve replacement, a commonly used term but a poorly understood one: dependency on definition and geometrical measurements. J Cardiovasc Comput Tomogr 2014;8:67–76.

56. Blanke P, Pibarot P, Hahn R, et al. Computed tomography-based oversizing degrees and incidence of paravalvular regurgitation of a new generation transcatheter heart valve. JACC Cardiovasc Interv 2017;10:810–20.

57. Popma JJ, Reardon MJ, Khabbaz K, et al. Early clinical outcomes after transcatheter aortic valve replacement using a novel self-expanding bioprosthesis in patients with severe aortic stenosis who are suboptimal for surgery: results of the evolut R U.S. Study. J Am Coll Cardiol Intv 2017;10:268–75.

58. Barbanti M, Yang TH, Rodès Cabau J, et al. Anatomical and procedural features associated with aortic root rupture during balloon-expandable transcatheter aortic valve replacement. Circulation 2013;128:244–53.

59. Barbanti M, Buccheri S, Rodés-Cabau J, et al. Transcatheter aortic valve replacement with new-generation devices: a systematic review and meta-analysis. Int J Cardiol 2017;245:83–9.

60. Urena M, Mok M, Serra V, et al. Predictive factors and long-term clinical consequences of persistent left bundle branch block following transcatheter aortic valve implantation with a balloon-expandable valve. J Am Coll Cardiol 2012;60:1743–52.

61. Piazza N, Onuma Y, Jesserun E, et al. Early and persistent intraventricular conduction abnormalities and requirements for pacemaking after percutaneous replacement of the aortic valve. J Am Coll Cardiol Intv 2008;1:310–6.

62. Franzoni I, Latib A, Maisano F, et al. Comparison of incidence and predictors of left bundle branch block after transcatheter aortic valve implantation using the corevalve versus the edwards valve. Am J Cardiol 2013;112:554–9.

63. Colombo A, Latib A. Left bundle branch block after transcatheter aortic valve implantation: inconsequential or a clinically important endpoint? J Am Coll Cardiol 2012;60:1753–5.

64. Calvi V, Conti S, Pruiti GP, et al. Incidence rate and predictors of permanent pacemaker implantation after transcatheter aortic valve implantation with self-expanding CoreValve prosthesis. J Intervent Card Electrophysiol 2012;34:189–95.

65. Aktug Ö, Dohmen G, Brehmer K, et al. Incidence and predictors of left bundle branch block after transcatheter aortic valve implantation. Int J Cardiol 2012;160:26–30.

66. Sinning JM, Petronio AS, Van Mieghem N, et al. Relation between clinical best practices and 6-month outcomes after transcatheter aortic valve implantation with CoreValve (from the ADVANCE II study). Am J Cardiol 2017;119:84–90.

67. Hamdan A, Guetta V, Klempfner R, et al. Inverse relationship between membranous septal length and the risk of atrioventricular block in patients undergoing transcatheter aortic valve implantation. J Am Coll Cardiol Intv 2015;8:1218–28.

68. Van Mieghem NM, Tchetche D, Chieffo A, et al. Incidence, predictors, and implications of access site complications with transfemoral transcatheter aortic valve implantation. Am J Cardiol 2012;110:1361–7.

69. Tamburino C, Capodanno D, Ramondo A, et al. Incidence and predictors of early and late mortality after transcatheter aortic valve implantation in 663 patients with severe aortic stenosis. Circulation 2011;123:299–308.

70. Basir MB, Velez C, Fuller B, et al. Rates of vascular access use in transcatheter aortic valve replacement: a look into the next generation. Cathet Cardiovasc Interv 2016;87:E166–71.

71. Svensson LG, Dewey T, Kapadia S, et al. United States feasibility study of transcatheter insertion of a stented aortic valve by the left ventricular apex. Ann Thorac Surg 2008;86:46–54; discussion 54–5.

72. Abu Saleh WK, Goswami R, Chinnadurai P, et al. Direct aortic access transcatheter aortic valve replacement: three-dimensional computed tomography planning and real-time fluoroscopic image guidance. J Heart Valve Dis 2015;24:420–5.

73. Okuyama K, Jilaihawi H, Kashif M, et al. Transfemoral access assessment for transcatheter aortic valve replacement: evidence-based application of computed tomography over invasive angiography. Circ Cardiovasc Imaging 2014;8.

74. Manunga JM, Gloviczki P, Oderich GS, et al. Femoral artery calcification as a determinant of success for percutaneous access for endovascular abdominal aortic aneurysm repair. J Vasc Surg 2013;58:1208–12.

75. Toggweiler S, Gurvitch R, Leipsic J, et al. Percutaneous aortic valve replacement: vascular outcomes with a fully percutaneous procedure. J Am Coll Cardiol 2012;59:113–8.

76. Hayashida K, Lefvre T, Chevalier B, et al. Transfemoral aortic valve implantation: new criteria to predict vascular complications. J Am Coll Cardiol Intv 2011;4:851–8.

77. Rodés-Cabau J, Webb JG, Cheung A, et al. Transcatheter aortic valve implantation for the

Descargado para Anonymous User (n/a) en Consejeria de Sanidad de Castilla y Leon(Sacyl) de ClinicalKey.es por Elsevier en marzo 05, 2019.
Para uso personal exclusivamente. No se permiten otros usos sin autorización. Copyright ©2019. Elsevier Inc. Todos los derechos reservados.

treatment of severe symptomatic aortic stenosis in patients at very high or prohibitive surgical risk. Acute and late outcomes of the multicenter Canadian experience. J Am Coll Cardiol 2010;55:1080–90.

78. Gleason TG, Schindler JT, Hagberg RC, et al. Subclavian/axillary access for self-expanding transcatheter aortic valve replacement renders equivalent outcomes as transfemoral. Ann Thorac Surg 2018;105:477–83.

79. Wee IJY, Stonier T, Harrison M, Choong AMTL. Transcarotid transcatheter aortic valve implantation: a systematic review. J Cardiol 2018;71:525–33.

80. Greenbaum AB, Babaliaros VC, Chen MY, et al. Transcaval access and closure for transcatheter aortic valve replacement: a prospective investigation. J Am Coll Cardiol 2017;69:511–21.

81. Andreini D, Pontone G, Mushtaq S, et al. Diagnostic accuracy of multidetector computed tomography coronary angiography in 325 consecutive patients referred for transcatheter aortic valve replacement. Am Heart J 2014;168:332–9.

82. Hamdan A, Wellnhofer E, Konen E, et al. Coronary CT angiography for the detection of coronary artery stenosis in patients referred for transcatheter aortic valve replacement. J Cardiovasc Comput Tomogr 2015;9:31–41.

83. Harris BS, De Cecco CN, Schoepf UJ, et al. Dual-source CT imaging to plan transcatheter aortic valve replacement: accuracy for diagnosis of obstructive coronary artery disease. Radiology 2015;275:80–8.

84. Opolski MP, Kim W-K, Liebetrau C, et al. Diagnostic accuracy of computed tomography angiography for the detection of coronary artery disease in patients referred for transcatheter aortic valve implantation. Clin Res Cardiol 2015;104:471–80.

85. Matsumoto S, Yamada Y, Hashimoto M, et al. CT imaging before transcatheter aortic valve implantation (TAVI) using variable helical pitch scanning and its diagnostic performance for coronary artery disease. Eur Radiol 2017;27:1963–70.

86. Rossi A, De Cecco CN, Kennon SRO, et al. CT angiography to evaluate coronary artery disease and revascularization requirement before transcatheter aortic valve replacement. J Cardiovasc Comput Tomogr 2017;11:338–46.

87. Leon MB, Piazza N, Nikolsky E, et al. Standardized endpoint definitions for transcatheter aortic valve implantation clinical trials: a consensus report from the Valve Academic Research Consortium. Eur Heart J 2011;32:205–17.

88. Kappetein AP, Head SJ, Généreux P, et al. Updated standardized endpoint definitions for transcatheter aortic valve implantation. J Am Coll Cardiol 2012;60:1438–54.

89. Salgado RA, Budde RPJ, Leiner T, et al. Transcatheter aortic valve replacement: postoperative CT findings of Sapien and CoreValve transcatheter heart valves. Radiographics 2014;34:1517–36.

90. Blanke P, Schoepf UJ, Leipsic JA. CT in transcatheter aortic valve replacement. Radiology 2013;269:650–69.

91. Symersky P, Budde RPJ, Prokop M, de Mol BAJM. Multidetector-row computed tomography imaging characteristics of mechanical prosthetic valves. J Heart Valve Dis 2011;20:216–22.

92. Willson AB, Webb JG, Labounty TM, et al. 3-dimensional aortic annular assessment by multidetector computed tomography predicts moderate or severe paravalvular regurgitation after transcatheter aortic valve replacement: a multicenter retrospective analysis. J Am Coll Cardiol 2012;59:1287–94.

93. Willson AB, Webb JG, Gurvitch R, et al. Structural integrity of balloon-expandable stents after transcatheter aortic valve replacement: assessment by multidetector computed tomography. J Am Coll Cardiol Intv 2012;5:525–32.

94. Binder RK, Webb JG, Toggweiler S, et al. Impact of post-implant SAPIEN XT geometry and position on conduction disturbances, hemodynamic performance, and paravalvular regurgitation. J Am Coll Cardiol Intv 2013;6:462–8.

95. Tan JS, Leipsic J, Perlman G, et al. A strategy of underexpansion and ad hoc post-dilation of balloon-expandable transcatheter aortic valves in patients at risk of annular injury favorable mid-term outcomes. J Am Coll Cardiol Intv 2015;8:1727–32.

96. Gooley RP, Cameron JD, Meredith IT. Assessment of the geometric interaction between the lotus transcatheter aortic valve prosthesis and the native ventricular aortic interface by 320-multidetector computed tomography. J Am Coll Cardiol Intv 2015;8:740–9.

97. Bekeredjian R, Bodingbauer D, Hofmann NP, et al. The extent of aortic annulus calcification is a predictor of postprocedural eccentricity and paravalvular regurgitation: a pre- and postinterventional cardiac computed tomography angiography study. J Invasive Cardiol 2015;27:172–80.

98. Schuhbaeck A, Weingartner C, Arnold M, et al. Aortic annulus eccentricity before and after transcatheter aortic valve implantation: comparison of balloon-expandable and self-expanding prostheses. Eur J Radiol 2015;84:1242–8.

99. Nishimura RA, Otto CM. AHA/ACC Focused Update of the 2014 AHA/ACC Guideline for the Management of Patients with Valvular Heart Disease: A Report of the American College of Cardiology/American Heart Association Task Force on Clinical Practice Guidelines; 2017. 2017.

100. Makkar RR, Fontana G, Jilaihawi H, et al. Possible subclinical leaflet thrombosis in bioprosthetic aortic valves. N Engl J Med 2015;373:2015–24.

101. Hansson NC, Grove EL, Andersen HR, et al. Transcatheter aortic valve thrombosis: incidence, predisposing factors, and clinical implications. J Am Coll Cardiol 2016;68:2059–69.

102. Yanagisawa R, Hayashida K, Yamada Y, et al. Incidence, predictors, and mid-term outcomes of possible leaflet thrombosis after TAVR. JACC Cardiovasc Imaging 2017;10:1–11.

103. Sondergaard L, De Backer O, Kofoed KF, et al. Natural history of subclinical leaflet thrombosis affecting motion in bioprosthetic aortic valves. Eur Heart J 2017:2201–7.

104. Landes U, Kornowski R. Transcatheter valve implantation in degenerated bioprosthetic surgical valves (ViV) in aortic, mitral, and tricuspid positions: a review. Struct Hear 2017;00:1–11.

105. Ribeiro HB, Rodés-Cabau J, Blanke P, et al. Incidence, predictors, and clinical outcomes of coronary obstruction following transcatheter aortic valve replacement for degenerative bioprosthetic surgical valves: insights from the VIVID registry. Eur Heart J 2018;39:687–95.

106. Blanke P, Soon J, Dvir D, et al. Computed tomography assessment for transcatheter aortic valve in valve implantation: the vancouver approach to predict anatomical risk for coronary obstruction and other considerations. J Cardiovasc Comput Tomogr 2016;10:491–9.

107. Bapat VN, Attia R, Thomas M. Effect of valve design on the stent internal diameter of a bioprosthetic valve: a concept of true internal diameter and its implications for the valve-in-valve procedure. J Am Coll Cardiol Intv 2014;7:115–27.

108. Suchá D, Daans CG, Symersky P, et al. Reliability, agreement, and presentation of a reference standard for assessing implanted heart valve sizes by multidetector-row computed tomography. Am J Cardiol 2015;116:112–20.

Descargado para Anonymous User (n/a) en Consejeria de Sanidad de Castilla y Leon(Sacyl) de ClinicalKey.es por Elsevier en marzo 05, 2019.
Para uso personal exclusivamente. No se permiten otros usos sin autorización. Copyright ©2019. Elsevier Inc. Todos los derechos reservados.